ON THE DAMPING ANALYSIS OF LAYERED BEAM STRUCTURES

A THESIS SUBMITTED IN PARTIAL FULFILLMENT OF THE REQUIREMENTS FOR THE DEGREE OF

Master of Technology

(By Research)

In

Mechanical Engineering

(Specialization: *Machine Design and Analysis*)

By

SAMRESH GARNAIK

Roll No.613ME3005

Under the supervision of

Prof. S.C. Mohanty

Associate Professor

Department of Mechanical Engineering

National Institute of Technology Rourkela

DEPARTMENT OF MECHANICAL ENGINEERING
National Institute of Technology Rourkela
(India)

2015

C E R T I F I C A T E

This is to certify that the thesis entitled ***On the damping analysis of layered beam structures*** submitted by **SAMRESH GARNAIK** to National Institute of Technology, Rourkela for the award of the degree of **Master of Technology (By Research)** in *Mechanical Engineering* (Specialization: Machine Design and Analysis) is an authentic record of research work carried out by him under my guidance and supervision.

The work incorporated in this thesis to the best of my knowledge has not been submitted to any other university or institute for the award of a degree or diploma.

Prof. S.C. Mohanty
Associate Professor
Department of Mechanical Engineering
National Institute of Technology
Rourkela

Acknowledgement

With all sincerity, I express my veracious thanks to National Institute of Technology, Rourkela for providing me the golden opportunity to work in this reputed organization. I am deeply indebted to Dr. S.C. Mohanty for his invaluable guidance. I express my gratitude to him for his heart whelming full support in making this compilation a magnificent experience which is very fruitful for shaping up my ideas and project report.

This project would not have been possible without the precious advice, proper tips and support from Mr. Srimant Kumar Mishra. This project would not have taken the present shape without his valuable guidance and his willingness to share his bright thoughts with me.

I am also benefitted by the outstanding works from all the instrument operators help with their particular skill in handling precisely delicate equipments.

I would like to acknowledge the support of Miss. K.V.Varalaxmi, Mr. Puneet Kumar, Mr. Prabhu Lakshmanan, Mr. Shince Joseph and Ms Madhusmita Senapati for their constant support during my study carrier.

I also want to thank my parents who inspired, encouraged and fully supported me in every step of my life by providing me not just financial, but moral and spiritual support.

Samresh Garnaik

Abstract

The present work deals with the improvement of damping capacity of layered bolted joint beam and sandwich beam with constrained viscoelastic layer. Damping capacity of structural element is an important design aspect. It enables to reduce the amplitude of vibration, increase the long-term reliability and fatigue life. So it is a great challenge for engineers and scientists to develop suitable damping improvement technique in the field of aerospace, automobile and other industrial applications. A lot of researches are going in this field. Damping offers an excellent potential for energy dissipation. Friction plays a vital role in energy dissipation in layered structure, which is greatly influenced by the roughness in between the layers. In this work the effect of surface roughness and bolt tightening torque on the damping capacity of layered bolted joint beams has been experimentally investigated. Based upon the experimental results, Taguchi principle and artificial neural network method have been applied to develop models to predict damping in bolted layered beam structures. The damping capacity in terms of modal loss factor has been studied for sandwich beams with constrained viscoelastic layer. The effect of core loss factor and core thickness on modal loss factor of the sandwich beam has been studied using finite element based model. Predictive models to estimate damping in sandwich beams have been developed applying Taguchi principle and artificial neural network method. Both Taguchi principle and artificial neural network method can be successfully applied to predict damping in layered structures.

TABLE OF CONTENTS

FIGURE NO. **LIST OF FIGURES** **PAGE NO.**

TABLE NO.	LIST OF TABLES	PAGE NO.

Chapter -1

Introduction

INTRODUCTION

Background

It is difficult to eleminate completely the vibration in a structural member like machine parts, building structure, automobile components and military equipment etc., but we can reduce the vibration level to some extend so that the longevity of the product increases and noise delivered by the system to the surrounding decreases. Lots of work have been done to minimize the vibration effect in various fields. Damping is one of the key sources to dissipate the vibrational energy level. So it has been an attractive point to work by many researchers.

In our real life when a structure is under some form of disturbance or initial condition, the structure responds to the initial events. After some time the structure slows down and stops vibrating. It has been observe that vibration naturally does not stay for a long period of time, after some time it comes to static condition. So it is conclude that there is a mechanism or interaction between structure and the external world. The mechanism which drains out the energy or dissipates the mechanical energy of the structure is called damping. So damping is an energy dissipation effect. There are various ways in which energy dissipation takes place, in some case it is converted to thermal energy, which is an irreversible process. Most of the damping belong to this category. Another dissipation is in the form of radiation, which is not in the form of thermal energy, but in the form of sound. Generally in a fluid medium (air, liquid) this type of damping takes place.

During vibration when the structure is loaded periodically, due to repeated altering loads internal stresses arise in the structure. There is a great chance of premature failure of the structure due to fatigue phenomenon. Every structure exhibits unique frequency during vibration that frequency is known as natural frequency. When the frequency of external excitation and natural frequency of the structure match, the amplitude of the structure is maximum and that is the condition of resonance, where the maximum amount of vibration is produced. So looking into the above characteristic, it is very much essential to evaluate the natural frequency of a structure and the types of response to a particular form of external excitation. In this way it can be predicted whether the structure can accomplish the required function or not and in addition, the dynamic conditions like variable stress, endurance limit, noise level etc. can be calculated easily. Hence fruitfulness of the structure is optimized and maintained. From many investigations, it has been seen that various structural parameters affect the dynamic response. So if any improvement of response or changes is required, then the structure will be modified in most economical and appropriate way. Sometimes the dynamic response of the structure is controlled by changing the damping of the structure.

So before attempting to reduce the vibration in the structural member it is very much essential to point out the cause of external excitation force. If it is artificial external force then it can be managed to some level by condition monitoring without affecting the productivity of machinery, but if it is natural it is very difficult to handle e.g. pressure and direction of wind blowing towards the building etc.. Hence, there is more emphasis on the redesigning of the structure. Now a day, in the cutting age technology, there have been a great demand for those types of smart structures, having light weight, corrosion resistance, high stiffness, high strength and high

damping. So instead of using bulky monolithic structure, those types of smart structure are used in various structural members. Demerits of the monolithic structure are also large, they are heavily weighted, flexibility is very less, bulky in nature and dissipation of energy is also less, which leads to low capable damping structure. In a practical structural problem situation, the demand of damping is high, so a large amount of energy should drain out. So in order to improve the damping , many smart techniques are adopted like viscoelastic layers, multi-layered sandwich structure, insert of elastic material in the parent structure, magnetic damping in the structural member, and layered jointed structure by means of fastener like rivet, bolt, weld etc..

When the layered structure move by some external exciting agent relative slip appears in between the layers, which leads to a rising of friction in the intermediate portion. This friction energy is dissipated in the form of heat, which increase the damping of the structure. In the built- up structure, joint plays a significant role on the friction in the interface slip region of the beam. Joints are essential parts of engineering structure, but it's hard to understand the complex behaviour of joint by many researchers. These have a key role to reduce the vibration level. In the link and joint portion it has been found that lots of dissipated energy, greatly affect the dynamic behaviour and natural frequencies of the system. In the interface shear of the joint, a large amount of energy is released, so in this way joint plays an excellent damping potential in the structural member. Beards [11] has find out that 90% of damping activity is produced due to joint only , so by appropriate designing of joint we can enhance the damping to some extent. There are other benefits of the joint also, it increases the flexibility of the structure and low material damping of the whole assembly is also reduced. So in all engineering structure, for enhancing the damping more focus is given to the various types of joints.

1.2 Motivation

Joints are integral parts of all types of engineering structure. They are fabricated by various means through riveted, welded, and bolted etc.. Their function is to clamp the whole assembly in a specified manner and generate some amount of pressure in the intermittent contact area of the mechanical system. It has been found that pressure in between the layers is parabolic in nature, maximum at the joint portion and decreases gradually from the influential jone. In bolted joint, pressure can be changed manually by changing the tightening torque so it is an effective way to change the dynamic behaviour of the structure. Many works related to bolted and riveted joints are carried out by taking non-uniform pressure in between the assembled layers. But a small amount of works has been done by considering uniform pressure. Riveted and welded joints are extensively used in various structural fields, their demerit is they exhibit constant pressure in the interface. We can't control the interface pressure so also the friction parameter. The degree of slip damping in a structure, which is directly caused by dry friction depends on such factors as joint forces (bolt tension) or torque applied, surface quality or surface roughness and nature of material etc.. This is associated with wear, surface erosion and deterioration of structural members. So this shows that slip damping is time dependent. But by making structure layer by layer we can reduce the deterioration, increase the level of energy dissipation, with a reliable amount of stiffness so that it withstands the loading condition. A few works have been reported on the effect of surface quality on the damping parameters in the layered structures which is the main motivation to focus on this field.

Apart from surface properties, dimensional properties like thickness, length, width, number of layers, the amount of torque applied to the joint, relative dynamic slip generated in the interlayer portion, amplitude and frequency of vibration etc. affect the energy dissipation process and many more concepts are to be explored in this area.

1.3 Beam theory

A beam is a reliable model for designing of many types of structural problems used in military, ship, aerospace and machine tools etc.. According to the dimensional point of view, beams are two types, one is thin beam and other is thick beam. In static and dynamic conditions, lots of process take place in a beam. For study and analysis purpose two types of beam theory are popularly used. One is Euler- Bernoulli beam theory and another is Timoshenko beam theory. Both theories differ from their assumption. In first one, plane of cross section is perpendicular to the neutral axis and in the second one there is a rotation of the plane with the neutral axis. For longer and stiffer beam Euler beam theory is generally used. But in case of short beam, Timoshenko beam theory is used, where cross-sectional dimension are not small as comparison to length of the beam due to which shear deformation and rotary inertia are taken in account. In this thesis Euler-Bernoulli beam theory or thin beam theory where the thickness of the beam is very less compared to the length of the beam has been considered.

1.4 Outline of the thesis

The work reported in this thesis is broadly divided into six chapters. The outline of all the chapters are given below:

Chapter-1: This chapter gives a basic idea about structural damping and its importance and motivation for the present investigation.

Chapter-2: This chapter contains the concerned literature review on various aspects of structural vibration analysis of layered jointed structures. Most of the previous research works are presented in the chapter. This chapter also gives a description of various topics like the need for damping, types of damping, mechanism of damping etc..

Chapter-3: It describes complete experimental procedure to find damping in layered bolted aluminium beam structure and the result evaluated from the experiment. It also gives a basic idea about Taguchi principle to optimize the experimental data. The basic concept and algorithm of ANN are also provided in the chapter.

Chapter-4: This chapter elaborates the details of analysis and prediction of damping in beam using Taguchi principle and ANN.

Chapter-5: This chapter gives the detailed investigation of sandwich beam with constrained viscoelastic layer with the help of finite element analysis. Modal loss factor is predicted using both Taguchi principle and ANN.

Chapter-6: Conclusion and scope of future work are reported in this chapter.

Chapter- 2

Literature survey

LITERATURE SURVEY

2.1 Introduction

For safe operation of the structural members, it is essential to study the vibrational behaviour of those members. The most popular objective of many problems is to suppress the unwanted vibration and identify the cause of vibration to improve product quality. A lot of works have been done to improve the damping capacity of structural members. As has been seen from the previous chapter, damping is the energy dissipation process. On layered bolted joint structures, lots of work have been done taking non-uniform and uniform pressure distribution in the interfacial region. But till now no work, on the basis of quantification of friction on the energy dissipation effect is notified. The present chapter elaborates details of investigation of cantilever layered bolted joint beam in the previous and current scenario.

2.2 Need of damping

Most of the structural members possess a very small amount of damping. Damping is the energy dissipation process, which mainly depends on the physical mechanism due to which it happens. The mechanism is a complex phenomenon, which is not easily perceived.

But without knowing the mechanism it is difficult to design structural members, where it produces unwanted vibration, noise, premature failure, fatigue problems etc. So in practical situation, like a crane hook is heavily damped to withstand the impact load, a machine tool is properly damped to smoothening the machining operation etc.

but it is not always true for all structural members needed for energy dissipation. So present research goal is to enhance the damping properties of bolted layered structure.

2.3 Types of damping

There are two ways in which drainage of energy takes place in built-up structures, one is active and other is passive way. In active way it needs an external power source to dissipate the energy, like sensor, actuator etc. But its demerit is it cannot be used in all cases due to power requirement, cost and environment etc.. For such conditions passive way is the reliable one. Various types of passive damping are viscous damping, viscoelastic damping, friction damping and impact damping etc.. Viscous and viscoelastic damping are temperature dependent [15], but friction damping work through a broad range of temperature. In passive way, jointed layer structure is the common way to dissipate energy. For simplicity damping is divided in two categories, (a) material damping and (b) structural damping.

2.3.1 Material damping

Material or internal damping is associated with the energy dissipation at the micro level to the molecular level. Generally it is caused due to microstructure defects, impurities inside the material, grain boundaries, thermoelastic effects, dislocation motion in metals and chain motion in polymers etc. [7]. This type of damping is not popular in structural fields due to its less damping capacity. There are two types of materials damping: hysteretic damping and viscoelastic damping. All kinds of internal damping exhibit the hysteresis loop curve. The relation between stress (σ) strain (ε) curves of a material is shown in Figure 2.1,

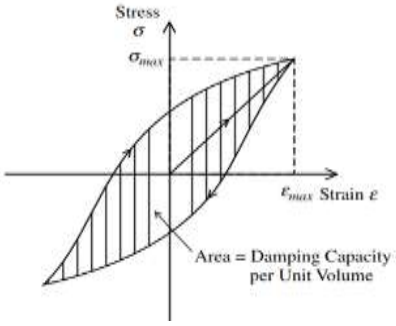

Figure 2.1 A typical hysteretic loop for mechanical damping [52]

shows the energy dissipated per unit volume of the material per stress cycle. Many investigation shows that when a material is critically stressed, energy is dissipated within the material. The energy dissipated in a cycle is independent of the frequency and it is approximately proportional to the stiffness and four times the amplitude of the vibration [6]. So internal damping belonging to this category is known as hysteric damping, and it is represented as specific damping capacity (Ψ) and is given by

$$\Psi = \oint \sigma \, d\varepsilon \tag{2.1}$$

Another type of internal damping is the viscoelastic damping. In this damping process stress of the material depend on the frequency of the strain which produces it. This means it depends on the frequency of the motion. There are lots of models to represent this phenomenon, kelvin-Voigt is a popular one [14]. This model is represented as in equation 2.2.

$$\sigma = E\varepsilon + E^* \frac{d}{dt}\left(\varepsilon(t)\right) \tag{2.2}$$

Where E is the young's modulus of elasticity, E^* is complex modulus, which is time independent. First term of the right hand side $E\,\varepsilon$ show the elastic behaviour of material and does not have any contribution to the damping of the material.

Second term of the right hand side contribute to the damping and this defines the damping capacity to unit volume as follow[14].

$$d_v = E^* \oint \frac{d}{dt}\left(\varepsilon(t)\right) d\varepsilon \tag{2.3}$$

2.3.2 Structural damping

Friction and rubbing between two surfaces are the major agents to dissipate energy in a mechanical system and cause structural damping [14]. The energy dissipation process depends on the physical process in which it occurs and the mechanism behind it. It varies from process to process, so there is no specific model to design it. But generally Coulomb-friction model is used to describe the dissipation effect where rubbing friction occurs. The overall energy dissipation is found out by finding the coefficient of restitution of two contacting bodies.

In a mechanical system structural damping shows the higher amount of damping than any other types of damping. Measured damping in a system displays the total quantity of the damping present in the structure, but subtracting other types of damping from total damping, the structural damping capacity is determined.

As discussed earlier in a friction joint, the structural damping is expressed by the best-suited Coulomb friction model, which is given in eq. 2.4

$$f = C\,\mathrm{sgn}(\dot{q}) \tag{2.4}$$

where,

f = the damping force

q = the relative displacement

C = friction parameters

and the signum function defined by:

Sgn(x) = 1 for x $\geq$0

Sgn (x) = -1 for x<0

2.3.3 Measurement of damping in structural members

There are different methods available to estimate damping. Basically these methods are divided into two major groups, one is time domain method, where response is a function of time and another is frequency domain method, where response is a function of frequency. Logarithmic decrement method, Step-response method and Hysteretic loop Method belong to time domain method. Magnification-factor method and Bandwidth method are belong to frequency domain method. Dealing with the logarithmic decrement method in time response is the common way to measure the damping [54].

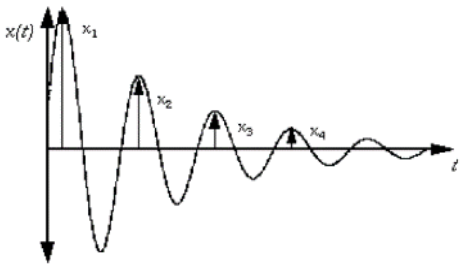

Figure 2.2 Response of a simple oscillator

Figure 2.2 shows the response when some initial excitation is given to the single degree of freedom system with viscous damping. The rate of successive decrease in amplitude of the response shows the extent of damping in measurement. The response of the curve is represented as follows

$$y(t) = y_0 \exp(-\zeta \omega_n t) \sin(\omega_d t) \qquad (2.5)$$

If amplitude of two successive peak is known then, logarithmic decrement (δ) finds out by the formula as shown in equation 2.6

$$\delta = \frac{1}{n}\ln\left(\frac{x_i}{x_{i+n}}\right) = \frac{2\pi\zeta}{\sqrt{1-\zeta^2}} \tag{2.6}$$

where, x_i is the amplitude at a i^{th} period of time and x_{i+n} is the amplitude after completion of n cycle, ζ is the damping ratio.

For small amount damping, the above equation is approximated as

$$\delta = 2\pi\zeta \tag{2.7}$$

Damping ratio present in the above equation is a dimensionless parameter, which represent the rate of decay of the curve during energy dissipation effects. From this parameter we can easily predict the dissipative effect of the structure by knowing the damping. It is the ratio of actual damping to critical damping of the structure.

The formula is $\delta = \frac{c}{\sqrt{2km}}$ (2.8)

where, c, k, m are the damping coefficient, stiffness, and mass respectively.

2.4 Improvement of damping capacity of the structure

Due to low material damping properties, lots of techniques are evolving to enhance the damping of the structural member. Energy dissipation is a major issue to recognise for designing of various types of structural members. Some of the techniques adopted for structural member are given below:

- Application of viscoelastic layer
- Layered jointed construction of structure

2.4.1 Application of viscoelastic layer

Viscoelastic material exhibits both characters of viscous material and elastic material, when it deforms due to any kind of external agent. Viscous material like honey, it opposes to shear flow of the motion, its strain is time dependent when some stress is applied to it. In case of elastic material hooks law is applied, it means strain is linearly proportional to the stress, where no dissipation of energy takes place. Combining two properties, we get a unique feature capable of elastic nature and viscous nature helping the damping effects. So for its unique feature, it is applicable in many structural applications. The modulus of viscoelastic material is always represented as a complex quantity .The real part of complex term is known as storage modulus (E_1), which is responsible for elastic behaviour and the imaginary part is known as loss modulus (E_2), which is for viscous behaviour and it shows the energy dissipative ability of the material. The formula of complex modulus is as shown in equation (2.9)

$$\eta = E_1 + E_2 i = \frac{\sigma}{e} e^{i\phi} \tag{2.9}$$

where, ϕ represent the phase angle between stress and strain of the viscoelastic material [53].

2.4.1.1 Constrained layer damping

The constrained layer structure is obtained by adding a damping layer to the base layer and then another constraining layer is clamped over it to form a sandwich structure. When the structure stretches due to any kind of vibration,shear strain arises in the middle layer. This leads to energy dissipation of whole structure due to the shear action of material without changing the longitudinal extension of the structure.

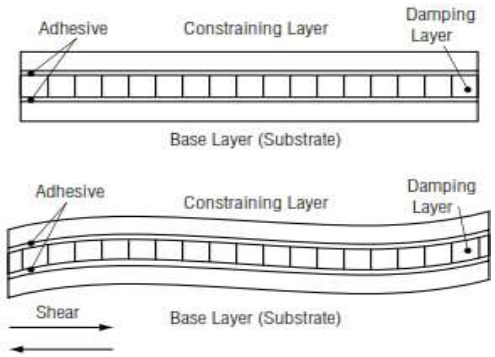

Figure 2.3 Constrained layer damping

This types of structure is also assembled by bolted or riveted joint instead of using adhesive in between the layer. Doing this, we get an adequate amount of surface to surface pressure in between the layer [40].

2.4.1.2 Unconstrained layer or external damping

It is the easiest form of material damping, where the damping material is placed over the base material with a strong bonding agent like some of the adhesives. Otherwise, it is dipped into hot liquefied material into the surface of the base layer, which hardens after cooling.

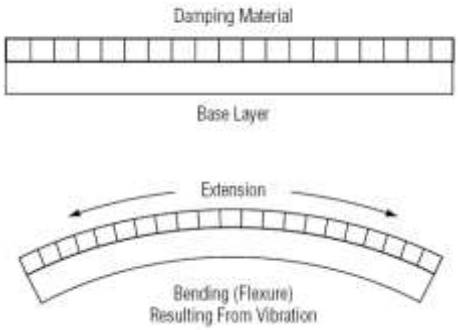

Figure 2.4 Unconstrained layer damping

During vibration, under the effect of bending stress, the extension and compression of the layers lead to the dissipation of energy from those structures. Damping increases

with the increase in damping layer thickness. Changing the composition of a damping material may also alter its effectiveness [27].

2.4.2 Layered jointed construction of structure

Control of unwanted vibration is a major issue in structural related problems. To overcome those problems research is going in the field of engineering and science. It is a benefit for a structural member to suppress the vibration to a reasonable limit and enhance the life of the structure. Assembling the beam type structures layer by layer and fabricating through various joints like riveted, welded, bolted makes them most damping capable. During vibration relative slip arises between the interfaces of layers, which produce friction, so energy dissipation. Friction is a complex nonlinear phenomenon that affect many parameters of the layered structure like interfacial pressure, types of joint, diameter of bolt or rivet, washer size etc.. These types of jointed structures are commonly used in various field like aerospace, building, heavy machinery, bridge construction and jet engine etc.. The current research work is mainly focused on the layered jointed structure, so as to increase the damping of the system.

2.5 Literature review on layered jointed built-up structures

Many built-in structures are connected by various types of mechanical joints. Such structure needs to have sufficient damping to slow down the excessive vibration. Generally, we found two types of damping on those structures. One is material or internal damping, other is structural damping due to joints. Internal damping, which is the inherent property of the material, is very low [5], but in structural damping, a large amount of energy is dissipated due to various types of joints [34]. In structural damping, joint plays an excellent role for energy dissipation. It is also estimated that

in case of bolted and riveted joint 90% of damping is due to joint only. Joints are the vital parameter to affect the friction produced in the layered structure [4,10,51,56].

Damping properties of the layered structure are improved by changing the thickness of the layers, increasing the number of layers and also changing the diameter of the bolt [3,41,46]. However attention is given to the spacing between the bolts to increase the damping. It has been found out that, jointed layered structure exhibit two types of motion, one is a micro slip and another is a macro slip. Most of the energy dissipated through the structure depends upon these types of motion. So it is better to understand the mechanism of these types of motion [12,32,37]. When the excitation force is low and slip is below some threshold range that types of slip is known as micro slip, but when the external excitation force is high and the slip in between the interface of the layers is high and above the threshold range, that type of motion is known as macro slip. Macro slip is hazardous to the structure, where a maximum portion of contact between the surfaces takes place, but in case of micro slip some amount of localising contact between the surfaces of the beam takes place, which is efficient to produce friction on the structure.so also the dissipation of energy [38,50].

Due to this type of activity, friction is a major agent to dissipate energy from the layer structure [9,15,18,19,21,22,25,31,45,47,55]. Nishiwaki et al. [52] and Masuko [44] found that energy dissipation in cantilever beam considering the micro slip and normal force at the interface. It was also found out a micro slip at the interface of the layered structure occurred when the optimum frictional load was reached. Ying et al. introduced a micro slip model to study the effects of friction at the joint at various dynamic responses.

Friction is a vital parameter for controlling the response of many engineering structures. In some case it produces desirable effects and some case it is undesirable. It is an opposing parameter in case of moving bodies, but in case of built up layered structure it is a very much crucial agent to dissipate energy. So designing a proper layered structure we can implement it in a field where huge vibration is produced like a big compressor parts in a power plant, nose and body parts of aircrafts, turbine and compressor parts of a jet engine etc.. Friction in the layered structure arises mainly due to relative motion between the layers, due to the transverse vibration. The most popular Coulomb law of friction model is generally used to describe the friction between two dry contact surfaces. In case of jointed layered structure, friction arises due to shear action between two contacting surface, tension due to a bolt or rivet and the material which they are made up off [57]. So joint friction in the built-up structure is the leading cause to dissipate more amount of energy [24,26,28,33,35,43,55]. Sandwich beam like structure having a viscoelastic material core has been extensively investigated to study its ability to control vibration. Kerwin [22] was the first person to carry out a quantitative analysis of the damping effectiveness of a constrained viscoelastic layer and he obtained a formula to estimate the loss factor. The general expressions of loss factors for uniform linear composites in terms of the physical properties of combined materials has been proposed by Ungar [20]**.** For a sandwich beam Ditaranto formulated a concept [42] to estimate natural frequencies, loss factor for specified length. Mead and Markus investigated the forced vibrational of three layered structure with viscoelastic core with diffirent bounadary conditions. They followed the method used by Ditaranto in their analysis. Rao in his work gave graphs and equations to evaluate resonant frequencies condition and loss factors for sandwich structure [17]. A fixed-fixed type sandwich cantilever structure with viscoelastic core

was examine by Asnani and Nakra [39]with different boundary conditions. The forced vibration response obtained by applying Ritz method matched well with their experimental results. Johnson and his co-workers workd on beams and plates with constrained viscoelastic layer using finite elemnt method [8] to find frequency and loss factor. Bhimaraddi explaind both the resonant frequencies and loss factors for a constrained layer damping using a model structure [2]. Banerjee investigated the free vibration of a sandwich beam implementing dynamic stiffness matrix method from which the frequencies and mode shapes were calculated. Sun et al. [13] established a finite element analysis to examine the effect of adding viscoelastic layer in damping and vibration control of composite laminates. Their theoretical results compared well with the experimental findings. Ha [30] suggested an exact analysis procedure for bending and buckling analysis of sandwich beam systems.

Avcar and Saplioglu [36] carried out a study to find natural frequencies of prismatic steel beam with various geometrical characteristics with four boundary conditions determined by artificial neural network in less period of time and also found that ANN gives better results than multiple regression models. Abuthakeer et al. [49] carried out an experimental analysis upon CNC lathe to control and predict vibration. They used a damping pad made of neoprene in the CNC lathe machine. From the factual experimental data, analysis of variance (ANOVA) technique is used to find the influential parameters on vibration. They found that natural frequency shift away from the operating frequency thereby avoiding the resonance condition of cutting tool. Chen et al. [23] studied artificial neural network model to forecast and classification of vibration in machine tools. They found that ANN technique is better technique than other classifier technique like SVM, Naive Bayes, DT classifier etc.. Aherwar et al. [1] carried out an experiment on vibration of carbon steel cutting tool for turning of

EN24 steel. They found that cutting speed has the maximum contribution on cutting tool vibration. Mohapatra [29] carried out experimental analysis and optimisation of process parameters like material removal rate and single pitch error of a spur gear machined by wire EDM. Parameters were successfully optimized using taguchi quality loss function.

2.6 Present work

The above literature study shows that the prediction and quantification of surface roughness on improving the damping capacity of the structural members have not been attempted. So also the optimum effectiveness of constrained layer damping treatments in enhancing the modal loss factor has not been studied. This forms the motivation for the present investigation. In this work the effect of surface roughness and bolt tightening torque on the damping capacity of layered bolted joint beams has been experimentally investigated. Based on the experimental results, Taguchi principle and artificial neural network method have been applied to develop models to predict damping in bolted layered beam structures. The damping capacity in terms of modal loss factor has been studied for sandwich beams with constrained viscoelastic layer. The effect of core loss factor and core thickness on modal loss factor of the sandwich beam has been investigated using finite element based model. Predictive models to estimate damping in sandwich beams have been developed applying Taguchi principle and artificial neural network method. Both Taguchi principle and artificial neural network method have been found to predict damping in layered structures, accurately.

Chapter 3

Experimental investigation

3

Experimental Procedure Details

3.1 Introduction

This chapter describes the experimental investigation of layered bolted jointed cantilever beam specimen, for estimation of structural damping. It also provides a testing procedure to measure the damping of layered aluminium beam specimen, by changing the roughness of connecting layers. The approach of the experiment is based on the Taguchi experimental design and prediction model motivated by the neural network system, which will be described in the later part of the thesis.

3.2 Specimen preparation

The specimens are prepared from commercial aluminium flat, by joining two number of layers, as shown in Figure 3.1 and 3.2. Equispaced bolt having nominal diameter of 4 mm are used to fabricate the structure in two number of layers. Washer of outer diameter 17 mm and inner diameter of 5 mm are used to distribute the pressure of nut over the surface of specimen so that surface is not damaged, and clamping action of the structure is more proficient. To generate diffierent level of micro contact in the structure, diffierent samount of torque is provided to the bolt.

Figure 3.1 Two layers bolted joint aluminium specimen (front view)

Figure 3.2 Two layers bolted joint aluminium specimen (side view)

The layered beam specimens are produced by maintaining different surface roughness in the interface layer. This is done by rubbing emery paper of different size 50, 60, 80, 100 to the work specimens. These are commercially available in the market, these are abrasive type papers used for the polishing operation. These paper are generally identified by their level of abrasiveness or grit number. Large grit size ranges from 40-50, which are usually used for removing a large quantity of paint and rust from the metal surface. Medium grit paper are designed in between 50-90 for a particular operation. When grit values exceed more than 90, finer paper with the least course is found.

After attending different roughness, the surface roughness of the specimen is measured by talysurf. In this experiment the instrument is Taylor Hobson talysurf which is a stylus and skid type of the device represented in the Figure 3.3. This device is operating on carrier modulating principle. The measuring point of this tool consists of the sharply pointed diamond stylus of 0.002mm tip radius, which is moved horizontal across the surface by means of the motorized driving unit. The stylus is made to trace the profile of surface irregularities, and the oscillatory movement of the stylus is converted to digital signal.

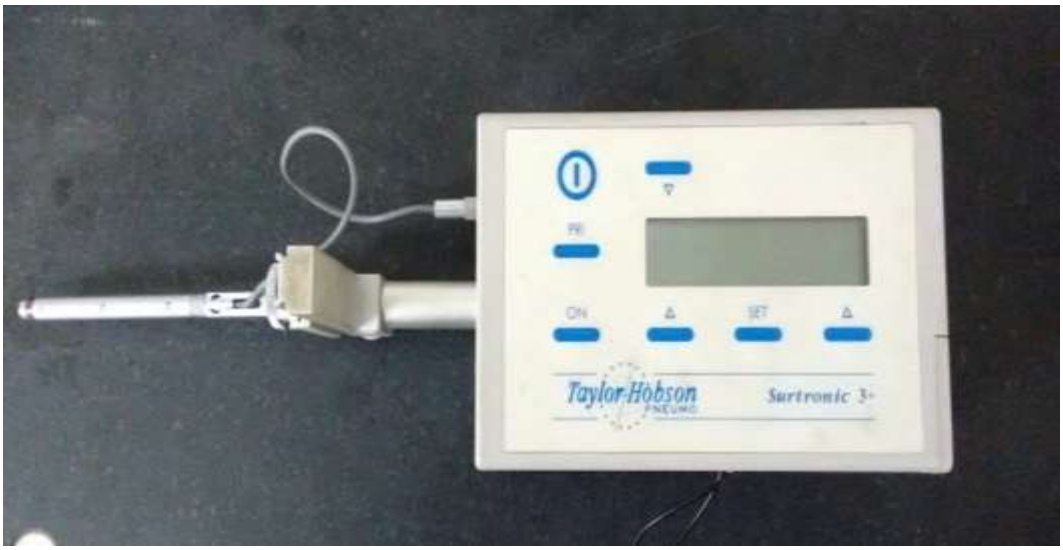

Figure 3.3 Taylor Hobson Talysurf used for measuring the roughness of beam specimen

The output of the instrument shows the roughness in the form of Ra, R stands for ‘roughness’ and a stands for ‘average’. The forms of roughness are also presented by this instrument is Rz, Rt, Rmax etc., but among them Ra is popularly used and in this work the indication of roughness in the form of Ra has been used. The average roughness (Ra) is the area that exist between the roughness profile and its mean line or the integral of the absolute value of roughness profile height over the span of profiles, which is shown in Figure 3.4.

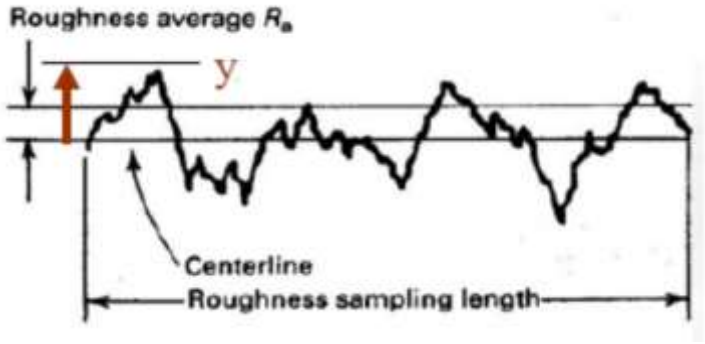

Figure 3.4 Measured roughness profile of the specimen

where, y is the ordinate of the profile and l is the sampling length. Average roughness (Ra) is represented mathematically as follows

$$R_a = \frac{1}{l}\int_0^l |y|\, dl = \frac{\sum_{i=1}^{n} y_i}{n} \tag{3.1}$$

After introducing a specific amount of roughness, the structure is fabricated in a layered way through bolted joints. The amount of interfacial pressure in the structure is proportional to the quantity of torque applied to the bolts. In this experimental analysis, different amount of torque is applied to the bolts to examine, how it affects the damping parameters. A clicking type adjustable torque wrench of MAC MASTER company make is used to set different amount of torque in the nut and bolts, which is shown in Figure 3.5.

Figure 3.5 A clicking type torque wrench

Specification of this instrument is

MAC MASTER Company
Model no TW-25
Range : 5-25 (lbt. Ft.) , 5-35(N.m) , .5-3.5 (kgf.m)
Least count 1

The maximum amount of recommended torque applied to the bolt fastener depends on the grade or quality of the fastener which is shown in Table 3.1, and the sockets which fit to different sizes of bolts are shown in Figure 3.6

Table 3.1 Different grade of bolt with nominal thread diameter

Normal thread dia. (mm)	4.6 Grade (Nm)	4.8 Grade (Nm)	5.6 Grade (Nm)	5.8 Grade (Nm)	6.6 Grade (Nm)	8.8 Grade (Nm)	9.8 Grade (Nm)	10.9 Grade (Nm)	12.9 Grade (Nm)	14.9 Grade (Nm)
3	0.57	0.76	0.71	0.95	0.85	1.5	1.7	2.1	2.6	3.0
4	1.3	1.8	1.7	2.2	2.0	3.5	4.0	5.0	6.0	7.0
5	2.7	3.6	3.3	4.5	4.0	7.1	8.0	10.0	12.0	14.0
6	4.5	6.1	5.7	7.6	6.3	12.1	13.6	17	20.4	23.8
7	7.6	10.2	9.5	12.7	11.4	12.1	13.6	17	20.4	23.8

Figure 3.6 Different size of socket used in torque wrench for different head size of bolt

To generate uniform contact throughout the structure, torque is kept constant for a set of experiment. Roughness is also varied from specimen to specimen. Details of the aluminium bolted cantilever structure is presented in Table 3.2.

Table 3.2 Details of aluminium bolted joint specimens with different roughness in the interface shearing area

Number of specimens	Number of layers	Dimension of the specimen (Width $\times$ Thickness of the layered beam($2h$)), where $h_1 = h_2 = h$	Diameter of connecting bolt(mm)	Number of bolt use	Length of beam (mm)	Washer size Outer dia.(D),Inner dia. (d) (mm)	Roughness of interface portion of layered structure (μm)
Specimen-1	2	25×3.8	4	10	640	17,5	1.08
Specimen-2	2	25×3.8	4	10	640	17,5	1.17
Specimen-3	2	25×3.8	4	10	640	17,5	1.41

3.3 Installation of experimental set-up

The schematic diagram of the experimental set-up and photographic view are shown in Figures 3.7 and 3.8 respectively. The end conditions are of cantilever type. In order to achieve it, the specimen end has to be bolted to a rigid fix frame. The base of the frame has been set on a concrete base so as to get maximum stability. A contact type mini accelerometer has been attached at the free end of the specimen and the other end of the accelerometer is attached to a digital storage oscilloscope. Then all required setting of the oscilloscope is done for the free vibration analysis.

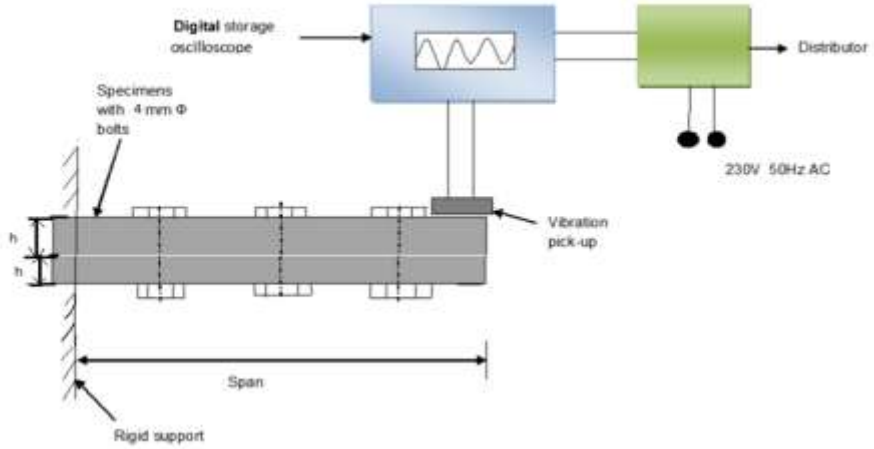

Figure 3.7 Schematic diagram of experimental set-up

Figure 3.8 Photographic view of experimental set-up

Then a small amount of excitation through tapping is provided to the layered specimen. Due to initial excitation the structure starts vibrating in the transverse direction. The vibration stays for a period of time and gradually diminishes. The electrical signal of decaying vibration process transmitted from beam specimen to digital oscilloscope device is recorded and stored. Once this graph is obtained the

parameters of the graph is calibrated to the amplitude versus time (second) to get the various parameters like natural frequency, damping parameters, time period of the cycle of vibration etc. Details of output signal obtained from oscilloscope for a two layered bolted structure specimen with a uniform torque of 12Nm in all bolts is shown in Figures 3.9 and 3.10 respectively.

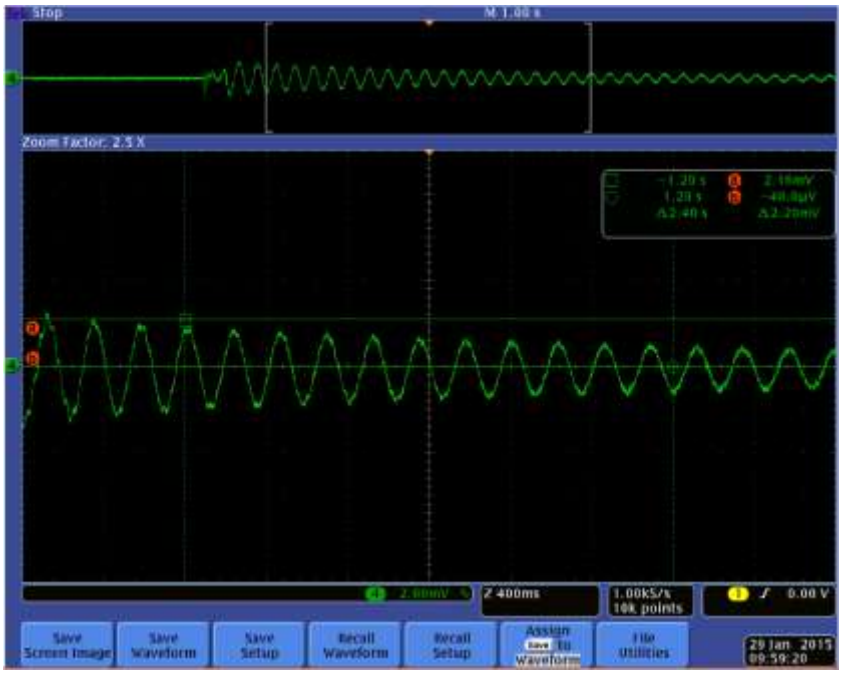

Figure 3.9 Time response of beam specimen.

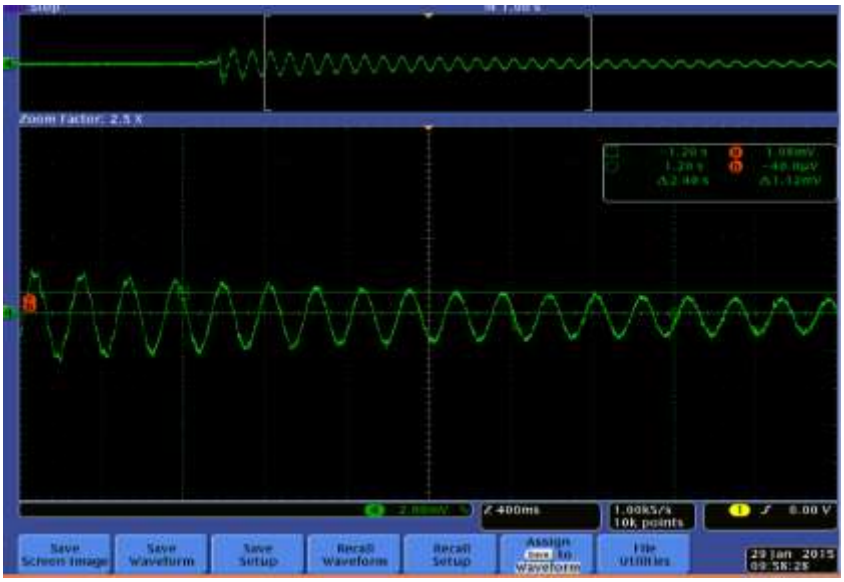

Figure 3.10 Time response of beam specimen.

The instruments that are used for experimental analysis are as follows:

- Digital phosphor oscilloscope
- Contact type accelerometer
- Distribution box

Digital oscilloscope

This is an electronic testing device that allows observation of frequently varying signal voltages, usually as a two-dimensional plot of one or more signal as a function of time. A non-electrical signal like sound, vibration also converted to voltages and displayed. As shown in Figure 3.11 it contains various input connector ports, control button on the panel to adjust the instrument to get the exact value.

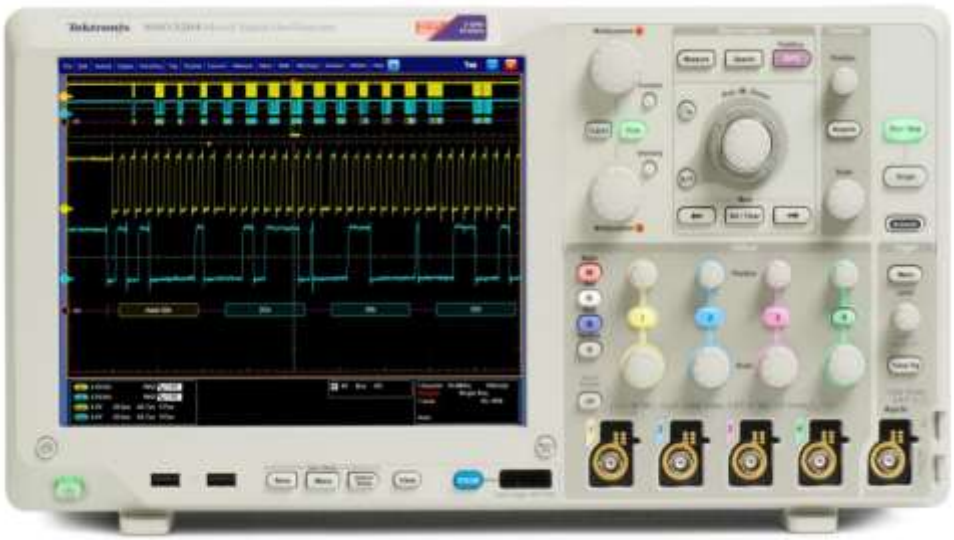

Figure 3.11 Digital phosphor oscilloscope

Specification:

Tektronix 4030 series digital phosphor oscilloscope

1 GHz to500 MHz bandwidths

Four channel to receive signal

Maximum range of Sample rates up to 5 GS/s on all channels

10 Mega point record length on all channels

264 mm XGA color display

USB drive available for quick and easy storage

Built-in Ethernet port support

USB 2.0 device port for direct PC control of the oscilloscope using USBTMC protocol

Contact type accelerometer

As accelerometer is a device that transforms the mechanical quantity, such as acceleration into an electrical signal , such as voltage or current. These are of various types such as contacting and non-contacting type. In the present work contacting type accelerometer used is shown in Figure 3.12. The accelerometer is attached to the vibrating surface and the other side is connected to connecting port of the storage oscilloscope.

Figure 3.12 A contact type accelerometer

Specifications:-

Type: - MV-2000.

Dynamic frequency range: - 2 c/s to 1000 c/s

Vibration amplitude: - ±1.5 mm max.

Coil resistance: - 1000Ω

Mounting: - by magnet

Dimensions: - cylindrical Length:-45 mm Diameter: - 19 mm

Weight: - 150 grams

Distribution box

AC supply of 230 volts and 50 Hz is provided to the oscilloscope for operating condition.

3.4 Measurement of logarithmic decrement and experimental evaluation

After getting the response curve from the oscilloscope, the data are analyzed and computed the various parameters like natural frequency, damping characteristic of the beam specimen. The signal visible as the output shows that the energy dissipation gradually increase with time. The response curve of the beam specimen is taken from the oscilloscope, and it is used for evaluation of the logarithmic decrement using the expression

$$\delta = \frac{1}{n} \ln \left(\frac{a_n}{a_{n+1}} \right) \tag{3.2}$$

where, a_n , a_{n+1} and n are the amplitude of the first cycle, last cycle and number of cycle respectively.This is done for a specimen with at a particular value of surface roughness. The tightening torque has been maintained uniform on each bolt to ensure uniform pressure distribution in the interface region on each set of the specimen. The different test results are shown in Table 3.3.

Table 3.3 Experimental test result of damping ratio and tightening torque for maintain different roughness of beam specimens.

Torque(Nm)	Damping ratio		
	Specimen-1	Specimen-2	Specimen-3
5	0.0137	0.01136	0.01981
7	0.0223	0.0142	0.0265
9	0.0232	0.01236	0.0365
11	0.1008	0.09168	0.12

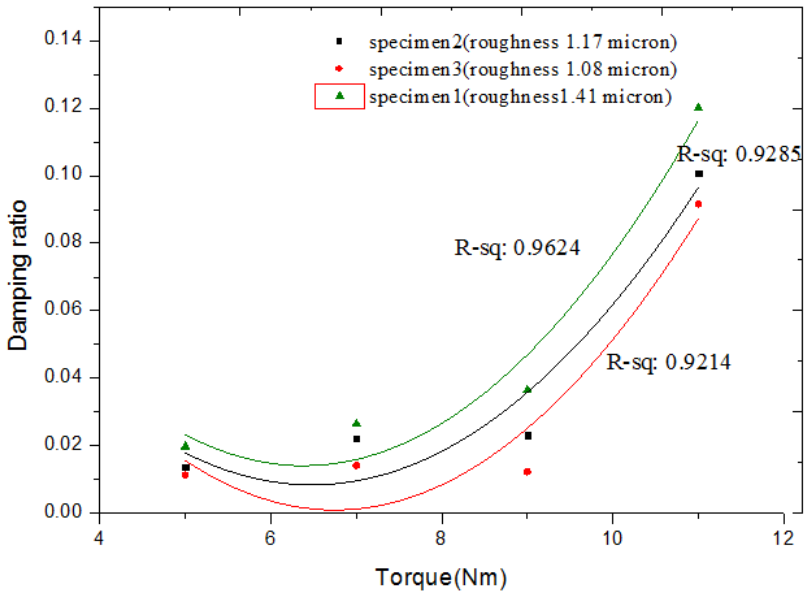

Figure 3.13 Variation of damping ratio with torque of a cantilever bolted beam specimen with different surface roughness.

Figures 3.13 and 3.14 depict the various experimental evaluation found from the recorded data taken by different reading from the oscilloscope. Figure 3.13 shows that with an increase in tightening torque the damping ratio of the structure increases after some initial drop with increase in tightening torque, and the rise of the roughness also

enhances the damping ratio of the structure.While Figure 3.14 displays, increase of natural frequency increases the damping ratio of the system which leads to improve the stiffness of the system. On the other hand decrease of roughness improves the flexibility of the system. The confirmation of the above result will be predicted and optimized through ANN and Taguchi concept in the next chapter.

Table 3.4 Experimental test result of damping ratio and natural frequency for maintaining different surface roughness .

	Damped time period (T_d) sec.	Natural frequency (Hz)	Damping ratio	Damped time period (T_d) sec.	Natural frequency (Hz)	Damping ratio	Damped time period (T_d) sec.	Natural frequency (Hz)	Damping ratio
Specimen-3 Roughness (1.08 micron)	0.2509	25.0313	0.0114	0.2414	26.018	0.014	0.2326	27.0	0.012
Specimen-2 Roughness (1.17 micron)	0.2511	25.0147	0.0135	0.2456	26.101	0.2	0.2331	26.9559	0.0231
Specimen-1 Roughness (1.41 micron)	0.2511	25.0202	0.02	0.2425	25.919	0.027	0.2340	26.8621	0.0400

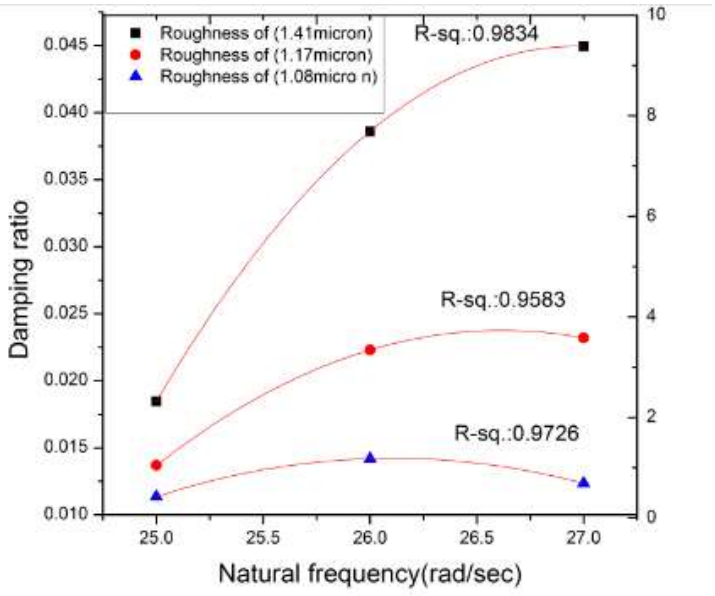

Figure 3.14 Variation of damping ratio with natural frequency of a cantilever bolted specimen with different surface roughness

3.5 Taguchi principle for experimental optimization

The primary aim to introduce Taguchi principle in this research work is to make a robust design and smooth conduct of my experimental work. It is a methodology for reducing the cost of designing process and time taken to complete the process. According to the inventor of this process, Dr. Genichi Taguchi, a healthy design is that which reduce the variability in process or product, while simultaneously guiding the performance to the optimum level.

Taguchi evaluation technique is based on to test a relationship between the sensitivity of response to the control parameter or independent variable. Generally a set of experiments is taken as an orthogonal array to targeting the optimal setting of control parameters. It provides the best setting to well-balanced the number of the experiments.

Generally for a set of experiments, various control parameters decide the values of target or response of the system. The technique which decide the best levels of process parameters to provide the output as the target value, such types of problem is known as “static problem’. This can be best explained using a P-Diagram, p meant for process or product.

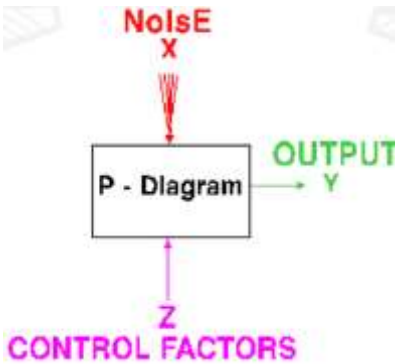

Figure 3.15 Product or process diagram of designing process

3.5.1 Signal to Noise (S/N) Ratio

There are three forms of signal to noise ratio (S/N) popularly used in many optimization techniques.

(1)Smaller-the-better:

This represents as

$$n = -10 \log_{10} [mean\ of\ sum\ of\ squares\ of\ measured\ data] \quad (3.3)$$

This is usually the preferred S/N ratio for all the disagreeable characteristics like "defects", "error "for which the ideal value is zero. In this case we have to minimize the mean and standard deviation.

(2) Larger-the-better:

This represented as

$$n = -10 \log_{10} [mean\ of\ sum\ of\ squares\ of\ \ reciprocal\ of\ measured\ data] \quad (3.4)$$

Increasing this S/N ratio is to maximize the mean and to minimize the standard deviation.

(3)Nominal-the-better:

This represented as

$$n = -10 \log_{10} [\text{square of mean/variance}] \quad (3.5)$$

This case is applied when, some specific value is most desired. It means neither a small nor a larger value is required.

Table 3.5 Parameter setting for free vibration damping in a layered beam specimen

Control factors	**symbols**	**Fixed parameters**	
Torque(Nm)	*A*	Length of specimen(mm)	640
		Width of specimen(mm)	25
		Thickness of two joint beams(mm)	3.8
Roughness(micron)	*B*	Nominal Dia. of bolt(mm)	4
		Outer Dia. ,inner Dia. (mm)	17,5
		Number of layers	2
		Number of bolt and washer	10,20
		Weight of whole structure(gm.)	232

Table 3.6 Control factors and selected levels (for damping analysis)

Control factors	level			
	I	II	III	UNIT
A:Torque	5	7	9	Nm
B:Roughness	1.08	1.17	1.41	μm

Table 3.7 Taguchi orthogonal array design (L9) for damping analysis

Test run	*A*(Torque)	*B*(Roughness)
1	1	1
2	1	2
3	1	3
4	2	1
5	2	2
6	2	3
7	3	1
8	3	2
9	3	3

3.6 Artificial neural network for prediction of experimental data

Energy dissipation process of the structural member is a nonlinear phenomenon as it depends on various parameters like friction, material properties, dimensional

properties, operating conditions etc. As mentioned before, to get the maximum amount of energy dissipation, appropriate operating parameters have to be planned so as to study their interrelated effects and predict the damping ratio as a response in a different condition. The damping analysis in an experimental way has a certain range, time-consuming, and is costly one. So to overcome these problems another smart technique namely artificial neural network (ANN) is applied to predict in a long range and complexity of damping behaviour.

The concept of an artificial neural network is derived from the human brain (nervous system), which consists of the massively parallel interconnection of a vast number of neurons. It archives different task like a perceptual task, recognition task etc. in a small fraction of time in an amazing way as a comparison to the high-performance supercomputer.

That's why researcher think if any computer can mimic the large amount of interconnection and networking exist between the nerve cells, can be utilized to do any complex task.

3.6.1 Some of the history of artificial neural network

McCulloch and Pitts (1943) are the first designers, who made a first model of the neural network system. They assembled much simple processing unit so that overall computation power is increased. They gave many ideas like a neuron has a threshold limit once that limit is reached, the neurons fire. It is still now the fundamental concept in which ANN operates, and those networks had a fixed set of weights. Hebb (1949) derived the learning rule that is if two neurons are active at the same time then their strength between them should be increased. In the year (1985-86) two fellow named as parker and LeCun discovered a learning algorithm for multilayer networks

called back backpropagation which solve lots of previous problems and also applied to solve problems those were not linearly separable.

3.6.2 Biological neuron model

The human brain is developed with a massively parallel network of 10 billion neurons and more than 60 trillion of interconnections, which makes the information process. Each cell is like a simple processing unit. An enormous interaction between the cells and their parallel processing unit makes brain's ability possible. The detaiied structure of the neurons is provided in Figure 3.16.

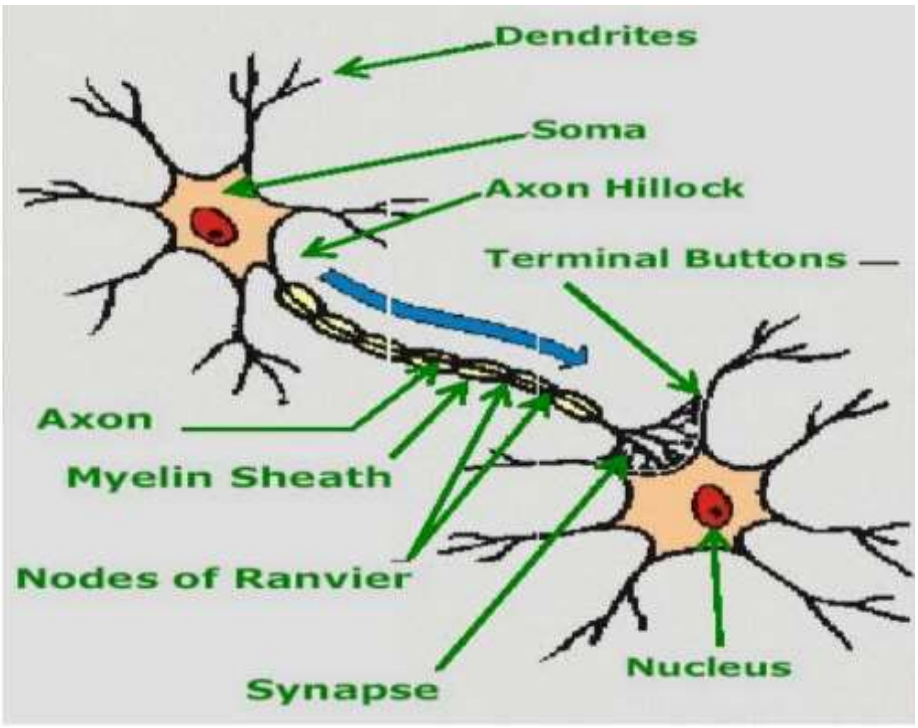

Figure 3.16 Structure of neurons [48].

Where, dendrite is the branch like structure prolonged from the cell body . The cell body contains a nucleus and other structures, which support chemical processing and production of neurotransmitters. Axon is a singular fibre which carries information from soma to synaptic sites of other neurons. Axon hillock is the site where all incoming information are summed up. Myelin sheath is composed of fat-containing

cells that insulate the axon from the electrical activity. This insulation helps to increase the rate of transmission of signals. Synapse is the point of connection between two neurons which transfer the information through by the means of electrochemical communication. The details flow of information in a neuron cell is shown in Figure 3.17.

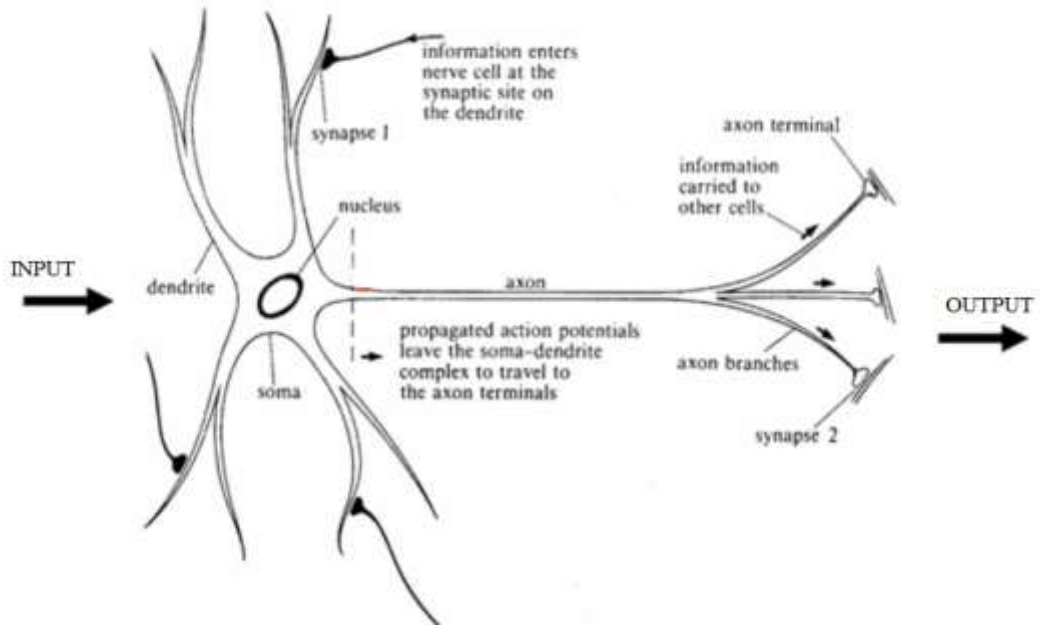

Figure 3.17 Transformation of information in neural cell [48].

3.6.3 Artificial neuron model

First McCulloch-Pitts introduced the simplified model of real neurons, known as threshold logic unit .Where

- A layer of input connections transports activations from other neurons.
- A processing unit sums the input data and applies it to a nonlinear activation function (transfer /threshold function).
- The output line triggers the result to other neurons.

In other words,

- The input to neurons arrives in the form of signals.
- The signal build up in cells.
- Finally the cell releases through the output.
- The cell can start processing signals again.

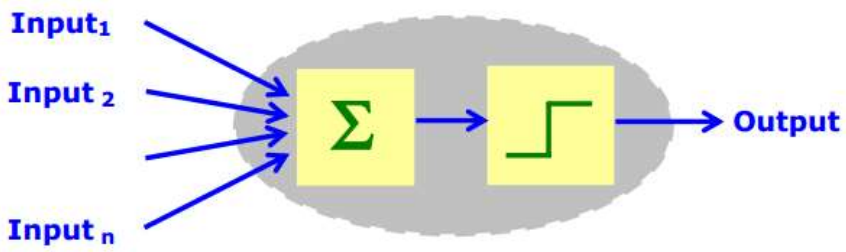

Figure 3.18 Simplified model of ANN

3.6.4 Basic elements of artificial neural networks

It consists of three basic elements weights, threshold and an activation function. The principles $W_1, W_2, \ldots W_N$ are synaptic weights to determine the strength of input vector $A = [A_1, A_2, \ldots\ldots, A_N]^T$ .Each input is multiplied by the connected weight of the neuron connection $A^T W$. The positive weight excites and the negative weight inhibits the node output.

$$\text{Input (I)} = A^T.W = A_1 W_1 + A_2 W_2 + \ldots\ldots\ldots + A_N W_N = \sum_{i=1}^{n} A_i w_i \qquad (3.6)$$

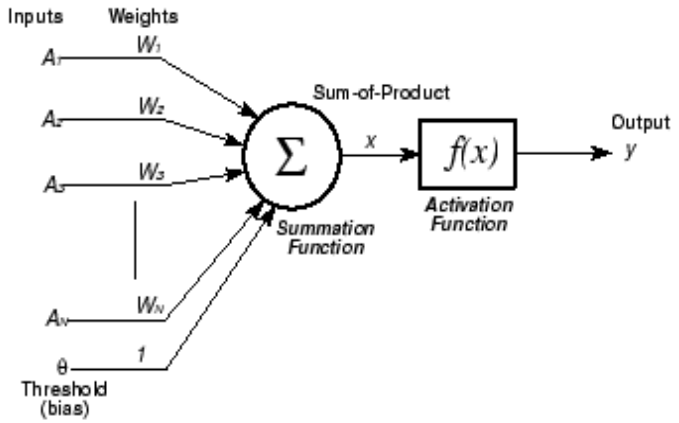

Figure 3.19 Basic elements of artificial neural network

In practice, the neurons do not fire (produce output) unless the total input goes beyond a threshold range. The total input gathering for each neuron is the sum of the weight inputs to the neuron minus the threshold value.

Then it is passed through a sigmoid function. The equation for the transition in a neuron is:

$$a = 1/ (1+\exp (-x)) \quad (3.7)$$

where

$x = \sum_{i=1}^{n} A_i w_i - Q$

a is the activation function of a neuron

A_i is the activation for neuron i

w_i is the weight

Q is the threshold subtracted

An activation function f is a mathematical function which operates the output of the signal. The most common types of activation function are linear function, threshold

function, piecewise linear function, sigmoidal(S-shaped) function, hyperbolic tangent function etc.. They are chosen according to the types of problem to solve the network. In this problem sigmoidal function is used for the better outcome result, which is shown in Figure 3.20.

This is written in the form of $y = f(I) = \frac{1}{1+e^{-\alpha I}}$ (3.8)

This is explained as

y = 0 as negative input values

y =1 as positive input values, with a smooth transition between two.

α is the slope parameter.

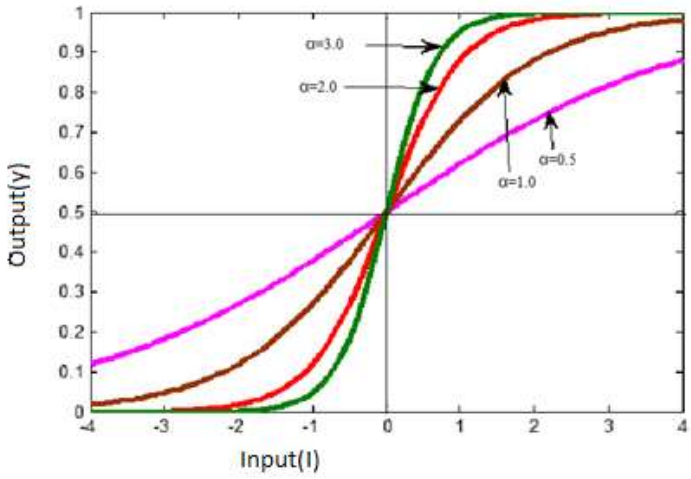

Figure 3.20 representation of sigmoidal function

3.6.5 Backpropagation Neural Network

It has been found that single-layer neural network has many restrictions. To overcome those problems, first time Minsky and papert (1969) found that these problems are solved by two layer feed forward network, but it did not give the solution how to adjust the weight from input to hidden layer. To solve this issue Rumelhart, Hinton and Williams in (1986) gave a beautiful idea, which says errors for the units of the hidden layers are evaluated by back-propagating the errors of the units of the output

layer. This method is popularly known as back-propagation learning rule. It can also be considered as a generalization of the delta rule for nonlinear activation function and multi-layer networks. It is a systematic method of training multi-layer artificial neural network as shown in Figure 3.21.

A backpropagation network consist of at least three layers of units:

- An input layer
- At least one hidden layer and
- An output layer.

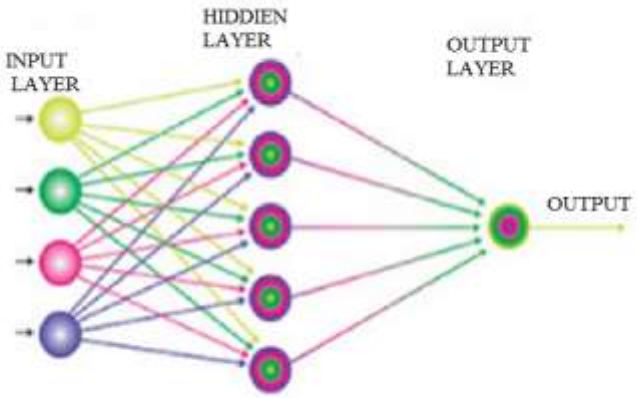

Figure 3.21 Multi-layer feed forward fashion

3.6.6 Backpropagation Learning Algorithm

Let us consider three layers of a network having '*l*' number of input nodes, hidden layer having *'m'* number of nodes and an output layer having '*n*' number of nodes. Sigmoidal function is considered as activation function for hidden layer and output layer and linear function for the output of input layer. The number of hidden layer chosen to lie between 1 and 21, [48].

The basic loop structure is given as follow [48]:

Initialize the weights

Repeat

For each training pattern

Train on that pattern

End

Until the error is acceptably low

Steps to Backpropagation Learning Algorithm BPN:

Step-1: Inputs and outputs are normalized with respect to their maximum values. It has been proven that neural networks work better if input-output lie between 0-1. For each training set, assume there are ' l ' inputs given by $\underset{lx1}{\{I\}_I}$ and 'n' outputs $\underset{nx1}{\{O\}_O}$ in a normalized form.

Step-2: Assuming number of neurons in the hidden layer to lie between 1<m<21.

Step-3: [V] represents the weights of synapses connecting inputs neurons and hidden neurons and [W] represents weights of synapses connecting hidden neurons and output neurons. Threshold value is taken as zero. Initialize the weights to small random value usually from -1 to 1.

$$[V]^0 = \text{[Random weights]}$$

$$[W]^0 = \text{[Random weights]}$$

$$[\Delta V]^0 = [\Delta W]^0 = [0] \tag{3.9}$$

Step-4: For training data we need to give one set of inputs and outputs. Present the pattern as inputs to the input layer $\{I\}_I$, then by using linear activation function,

The output of input layer is calculated as follows

$$\underset{lx1}{\{O\}_I} = \underset{lx1}{\{I\}_I} \tag{3.10}$$

Step-5: Then evaluating inputs to the hidden layer by multiplying corresponding weights of synapses as

$$\underset{m\times 1}{\{I\}_H} = \underset{m\times l}{[V]^T}\ \underset{l\times 1}{\{O\}_I} \tag{3.11}$$

Step-6: Compute the output of hidden layer units using sigmoidal function

$$\{O\}_H = \underset{m\times 1}{\left\{\begin{array}{c} . \\ . \\ \dfrac{1}{(1+e^{-I_{Hi}})} \\ . \\ . \end{array}\right\}} \tag{3.12}$$

Step-7: Then evaluating inputs to the outputs layers by multiplying corresponding weights of synapses as

$$\underset{n\times 1}{\{I\}_O} = \underset{n\times m}{[W]^T}\ \underset{m\times 1}{\{O\}_H} \tag{3.13}$$

Strep-8 Compute the output of output layer using sigmoidal function as follow

$$\{O\}_O = \begin{Bmatrix} . \\ . \\ \dfrac{1}{(1+e^{-I_{Oj}})} \\ \\ \end{Bmatrix} \tag{3.14}$$

The above is the output of network.

Step-9: Compute the error using difference between the network output and the desired output as for the j[th] training set as

$$E^P = \frac{\sqrt{\Sigma\left(T_j - O_{Oj}\right)^2}}{n} \tag{3.15}$$

Step-10:

Find the term {d} as

$$\{d\} = \begin{Bmatrix} . \\ . \\ \left(T_K - O_{OK}\right) O_{Ok}\left(1 - O_{Ok}\right) \\ . \\ . \end{Bmatrix}_{n\times 1} \tag{3.16}$$

Step-11: Find $[Y]$ matrix as

$$\underset{m\times n}{[Y]} = \underset{m\times 1}{\{O\}_H} \underset{1\times n}{\langle d \rangle} \tag{3.17}$$

Step-12: Find $\underset{m\times n}{[\Delta W]^{t+1}} = \underset{m\times n}{\alpha[\Delta W]^t} + \underset{m\times n}{\eta[Y]}$ (3.18)

Step-13 Find $\underset{m\times 1}{\{e\}} = \underset{m\times nn\times 1}{[W]}\{d\}$ (3.19)

$$\underset{1\times n}{\left\{d^*\right\}} = \begin{Bmatrix} . \\ . \\ e_i(O_{Hi})(1-O_{Hi}) \\ . \\ . \end{Bmatrix} \tag{3.20}$$

Find $[X]$ matrix as $\underset{1\times m}{[X]} = \underset{l\times 1}{\{O\}_I}\underset{1\times m}{\langle d^*\rangle} = \underset{l\times 1}{\{I\}_I}\underset{1\times m}{\langle d^*\rangle}$ (3.21)

Step-14: Find $\underset{1\times m}{[\Delta V]^{t+1}} = \alpha\underset{1\times m}{[\Delta V]^t} + \eta\underset{1\times m}{[X]}$ (3.22)

Step-15: Find $[V]^{t+1} = [V]^t + [\Delta V]^{t+1}$ (3.23)

$$[W]^{t+1} = [W]^t + [\Delta W]^{t+1}$$

Step-16: Find error rate as Error rate $= \dfrac{\sum E_p}{nset}$ (3.24)

Step-17: Repeat the steps 4 to 16 until the convergence in the error rate is less than the tolerance value.

End Algorithm BPN

Chapter -4

Prediction of damping in layered bolted joint beam structure

4

INVESTIGATION OF DAMPING IN LAYERED BOLTED JOINT BEAM

4.1 Damping test result and Taguchi analysis

The damping ratio and natural frequency of two-layer aluminium structure with changing torque and roughness with different test run condition from the experimental analysis are given in Table 4.1. The primary objective in structural vibration is to release more amount of energy and the structure should be robust in nature. In the damping analysis of layered structure, the two control variables as torque and roughness respectively, and the two response variables are damping ratio and natural frequency respectively. From the damping ratio one can estimate the energy dissipation effect. There are two responses of the system and it is requred to maximize the both to get a better outcome. There are many optimisation techniques available to find the multi-objective optimum parameters. Taguchi quality loss function is one of them, where the goal is to minimize the loss and present the result nearer to the target value. The steps to optimization of experimental data in Taguchi quality loss function are as follows :

Step-1: Find the quality loss function :

Consider for the responses, For lower the better :

Quality loss function $(L_{ij}) = Y_{ij}^{\,2}$ (i.e square of the responses) (4.1)

For higher the better :

Quality loss function $(L_{ij}) = 1 / Y_{ij}^{\,2}$ (4.2)

Where, Y_{ij} = ith performance of the response table in jth trial.

In the present problem both responses come under higher the better principle. So quality loss function for both the responses are calculated and presented in Table 4.2.

Table 4.1 Experimental results for different test run condition

SR NO.	Input		Out put	
	Torque (Nm)	Roughness (Micron)	Damping ratio (Dimensional less)	Natural frequency (Rad/sec)
1	5	1.08	0.01136	25.1810
2	5	1.17	0.0137	25.000
3	5	1.41	0.01981	25.05
4	7	1.08	0.0142	25.8101
5	7	1.17	0.0223	25.9974
6	7	1.41	0.0265	25.3089
7	9	1.08	0.01236	25.2105
8	9	1.17	0.0232	26.2030
9	9	1.41	0.0365	25.85163

Table 4.2 Quality loss function for damping ratio and natural frequency

SR NO.	Damping ratio	Natural frequency
1	7748.958	0.001577
2	5327.934	0.0016
3	2548.1855	0.001594
4	4959.333	0.001501
5	2010.8990	0.00148
6	1423.994	0.001561
7	6545.8049	0.001573
8	1857.907	0.001456
9	750.609	0.001496

Step-2 Calculation of normalized values

Normalized value of response data $(N_{ij}) = L_{ij} / L^{*}$ (4.3)

Where, L^{*} =maximum value of L_{ij}, Here L^{*} for the damping ratio is 7748.958 and for natural frequency 0.001577. The normalized value of both response data is shown in Table 4.3.

Table 4.3 Normalized values of damping ratio and natural frequency

SR NO.	Damping ratio	Natural frequency
1	1	1
2	0.6874	1.014585
3	0.3288	1.01078
4	0.6399	0.951807
5	0.25950	0.938491
6	0.18376	0.989854
7	0.844733	0.997464
8	0.23977	0.923272
9	0.0968	0.948637

Step-3 Calculation of total loss function

Total loss function $T_{ij} = \sum_{i=1}^{n} W_i N_{ij}$ (4.4)

Here is the weight given to the response variable, for this problem it is assumed that weight given to each response is 0.5. So we can evaluate the total quality loss function by taking an average of both normalized responses values. The total quality loss function is also known as multi-parameter characteristic index (MPCI), which gives combined effect of damping ratio and natural frequency of the system.

Table 4.4 Damping test result with corresponding total loss function and S/N ratios

SR NO.	Total loss function (T_{ij})	Signal to noise ratio (S/N) db.
1	1	0.00000
2	0.8509925	-1.40149
3	0.66979	-3.48123
4	0.7958535	-1.98334
5	0.5989955	-4.45153
6	0.586807	-4.63009
7	0.9210985	-0.71388
8	0.581521	-4.70869
9	0.5227185	-5.63464

After computation of total quality loss function, all training set of experimental data are transformed into signal-to-noise (S/N) ratio in the Table 4.4. There are many forms of signal to noise ratio depending upon their characteristics. The signal to noise

ratio for maximum damping ratio and natural frequency are coming under larger is the better characteristics and can be calculated as logarithmic transformation of loss function as shown below

$$S/N = -10\log(\sum(1/Y^2)/n) \tag{4.5}$$

where, n is the number of observations and Y the observed data.

The overall mean of signal to noise ratio of the system is found to be -0.626071 dB. The analysis is made using the popular software used for the design of experiment application known as MINITAB 17 and Figure 4.1and 4.2 show graphically the effect of the two control factors on damping ratio and natural frequency respectively.

The S/N ratio response is given in Table 4.5, from which it can be concluded that among all the factors, roughness is the most significant factor followed by torque in the bolted aluminium structure. It also leads to the conclusion from Figure 4.1 torque of 9 Nm and roughness of 1.41micron combination gives the maximum damping ratio in the structure, and from Figure 4.2 combination of 1.17micron roughness and 9Nm torque gives the maximizing condition for natural frequency.

Table 4.5 Response table for signal to noise ratios

Level	Roughness(*A*)	Torque(*B*)
1	-0.8991	-1.6276
2	-3.5206	-3.6883
3	-4.5820	-3.6857
Delta	3.6829	2.0607
Rank	1	2

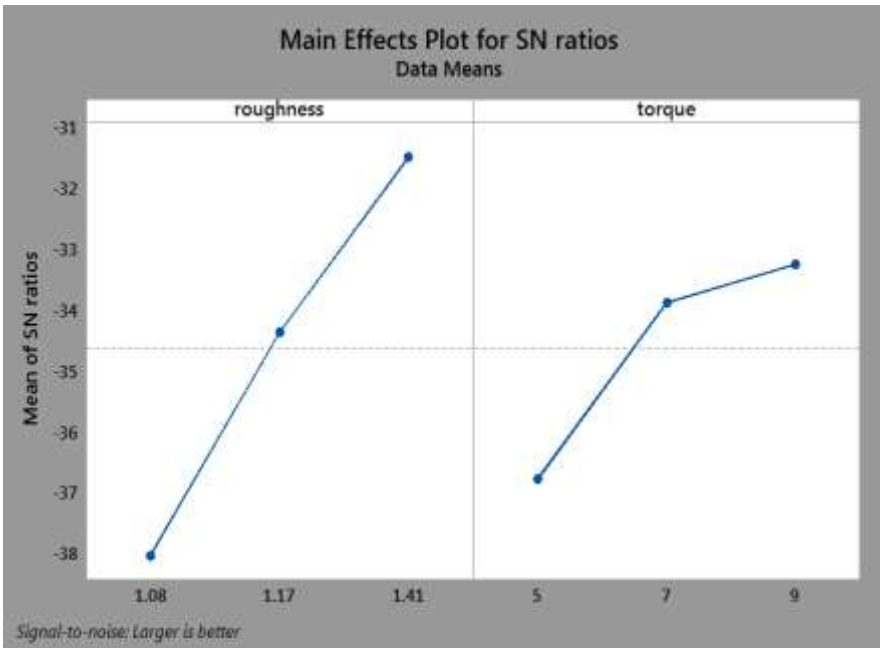

Figure 4.1 Effects of control parameters on damping ratio

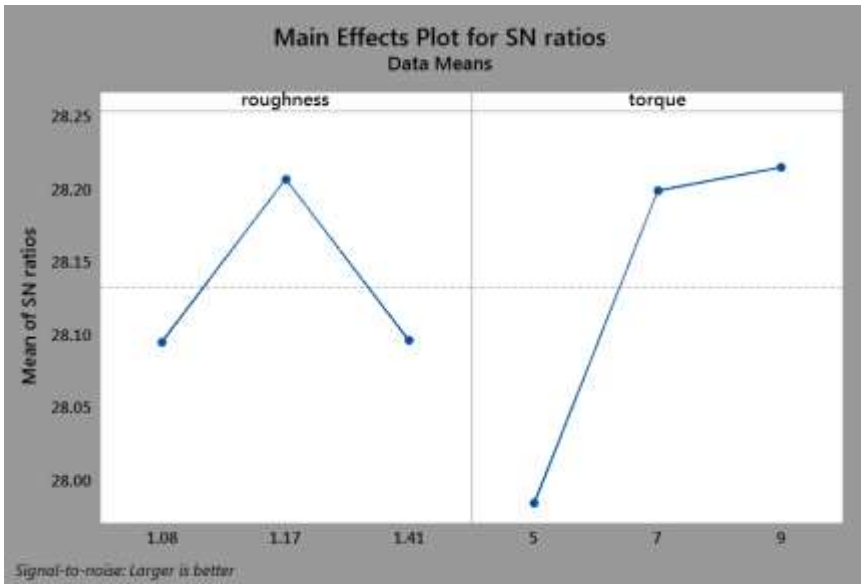

Figure 4.2 Effects of control parameters on Natural frequency

Table 4.6 Analysis of variance (ANOVA) for damping test result

Source	Degree of freedom	Sum of squares	Mean square= Sum of squares/degree of freedom	F-Value	P-value
Torque	2	0.05978	0.029891	6.73	0.052
Roughness	2	0.15696	0.078478	17.67	0.010
Error	4	0.01776	0.004441		
Total	8	0.023450			

Different factors affect the damping phenomena in different degree. A better feeling for relative effects of different factors is obtained by decomposition of the variance, which is commonly known as analysis of variance (ANOVA). Table 4.6 shows the anova table for damping response. The important information obtained here is the percentage influence of all factors over responses. P value less than 0.0500 indicate the model terms are significant.

In this case roughness and torque are both significant model terms. But roughness is more significant because of its higher variance ratio. So it shows roughness has more contribution to damping ratio.

4.2 Formulation of factors for maximum damping ratio and natural frequency

A regression model is proposed in the present work to develop the relationship between the input parameters such as roughness and torque with the output characteristics such as damping ratio and natural frequency. This model is developed by using popular statistical software SYSTST 13. The mathematical formulation to make a correlation among parameters in different order are given below.

1st order $P_f = K_0 + K_1 A + K_2 B$ (4.6)

2nd order $P_f = K_0 + K_1 A + K_2 B + K_3 A^2 + K_4 B^2$ (4.7)

where, P_f represents performance of the system

K_i (0, 1, 2, 3 and 4) are model constant

A is the torque in Nm

B is the roughness in micron

1st order ξ = -0.048 +0.002A +0.043B (R-sq-92.7%) (4.8)

2nd order ξ = -0.282 +0.008A +0.393B-0.*001*A^2-0.*139*B^2 (R-sq-98%) (4.9)

1st order ω_n =24.663+0.170A-0.276B (R-sq-99.98%) (4.10)

2nd order ω_n =-2.563+1.183A+38.295B-0.*072*A^2-15.*376*B^2 (R-sq- 99%) (4.11)

From equation 4.8 to equation 4.11, ξ and ω_n represent the performance output as damping ratio and natural frequency respectively in different order system. A and B term of the above equation show the torque and roughness of the system. The constants are calculated by regression analysis. The correctness of the correlation is also confirmed as high Coefficient of determination (R-sq.) is obtained from equation 4.8, 4.9, 4.10 and 4.11 as 92.7%, 98% 99.98% and 99% respectively. Therefore the model is quite appropriate to use for the additional predictive purpose.

4.3 Analysis and prediction of damping test result using Artificial Neural Network system:

As it is already mentioned, artificial neural network (ANN) is a technique which encompasses a training database to predict input-output evaluations. In this attempt our focus is to simulate damping ratio on different operating conditions of layered aluminium bolted structure. Here back-propagation learning algorithm is used to simulate the damping characteristics, which is based on the root mean square error criterion with supervised learning process. One structure is selected to optimize the damping ratio as shown in Figure 4.3. It consists of three layers as input layer, hidden layer and output layer.

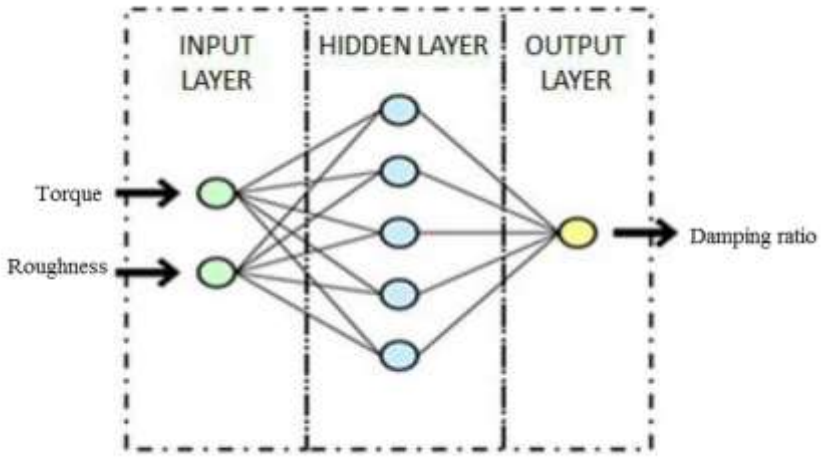

Figure 4.3 The structure of multilayer neural network system

In the above structure one set of torque value and another set of roughness value is given to the input layer, number of hidden layer assign to the structure in arrange of 1 to 21 and another set of output is assign to output layer.

The neural network works on the trial and error method of creating networks and examines functional input as well as output data. The network input data is estimated by the learning process to arrive a desired solution or prediction, whereas a required output is the solution or prediction that the neural network will be learning to produce using their relative importance of weight. It estimates and associates with the estimated value with the actual answer in the database.

At the first time neural network makes mistake as human being does. It rectifies mistakes by changing its weight in each iteration of the process. Repeatedly the network recalculate the data. This process goes on until the error converges to user-defined target value. A well trained skilful network is obtained once the network is sufficiently adopted at the study of the given data. After this, the user can provide a new data to the expert network to make a prediction based on his previous knowledge from the initial data base. So lots of inputs parameters like number of neurons in hidden layer, learning rate, momentum coefficient, number of iteration are provided to the network in each session to check the convergence of the error to predefined value. In the present problem below 10% error is given in between the predicated value and experimental value. A number of sessions are run to reach the target error, and this is shown in Table 4.7, and it is found that session 1 is the best training condition among all the sessions.

Table 4.7 Design of neural network and training parameters for all sessions, with two input and one output parameter

Session	# of neurons in input	# of neurons in hidden	# of neurons in output	Learning rate	Momentum coefficient	# of example set used in	# of epoch	Root mean Square
1	2	5	1	0.05	0.006	39	50000	0.009607
2	2	6	1	0.03	0.006	39	50000	0.009913
3	2	7	1	0.04	0.006	39	50000	0.009779
4	2	4	1	0.06	0.006	39	50000	0.009912
5	2	8	1	0.06	0.004	39	50000	0.00913
6	2	6	1	0.07	0.06	39	50000	0.009876

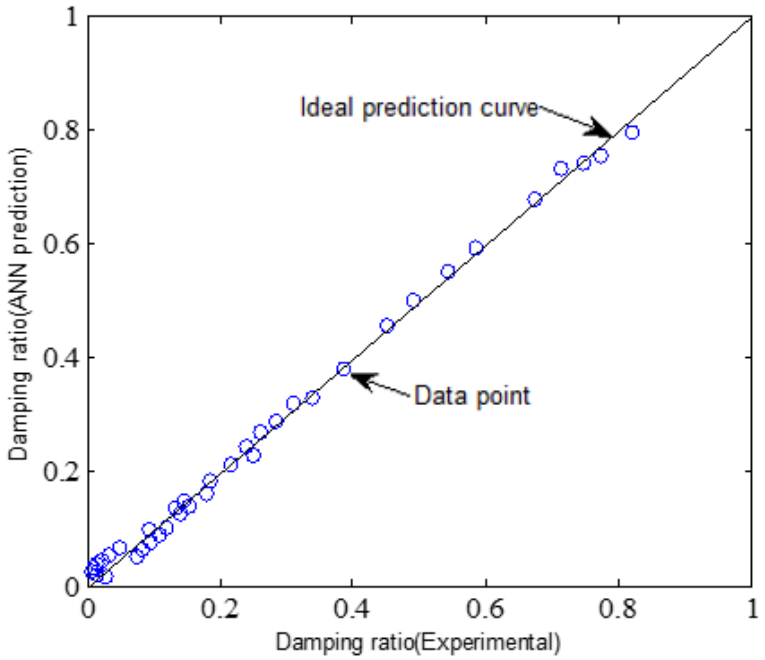

Figure 4.4 Validation curve for experimental and artificial neural network values.

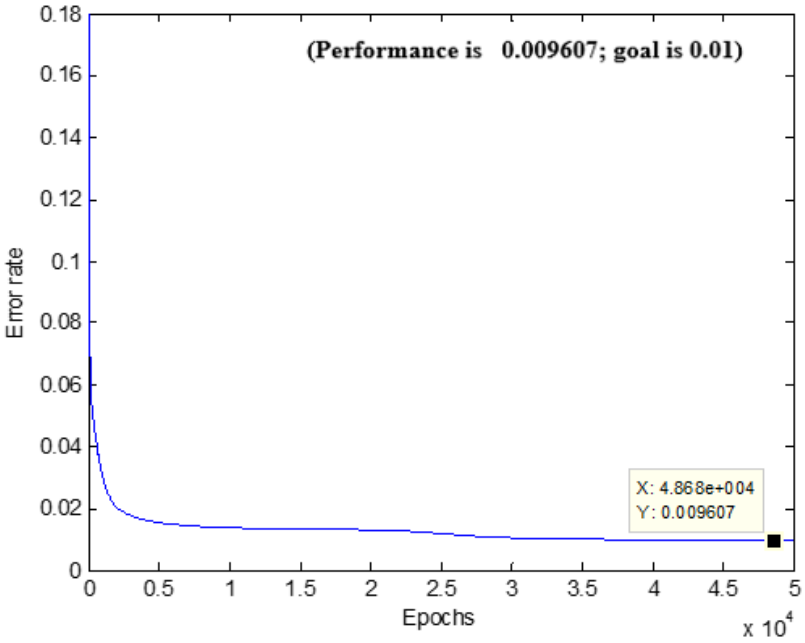

Figure 4.5 Error convergence curve with number of iteration.

After training a number of times, the network validate the prediction results with the experimental results, which is depicted in the Figure 4.4. It is seen from the figure, most of the data are very much nearer to the ideal prediction curve. Figure 4.5 shows that error rate decreases rapidly below 5000 iteration and convergence to 0.009607 at 50,000 iteration, which is nearer to our goal 0.01 of root mean square error. Lastly adjusted weight from Table 4.8 and 4.9 are used for testing further data to predict the damping ratio, and it is found that the error is below 4%, which is quite acceptable to adopt the model.

Table 4.8 Adjusted hidden weight (*V*)

-0.2143	-3.3083	0.2070	0.2084	0.2067	0.2092	0.2108
3.2309	3.8067	-3.1487	-3.1640	-3.1456	-3.1732	-3.1926

Table 4.9 Adjusted hidden weight (*W*)

18.5159
-18.6561
-16.2832
-16.5775
-16.2232
-16.7579
-17.1422

Similarly changing the architecture of neural network again damping ratio is calculated taking control variable as roughness and natural frequency, which is shown in Figure 4.6 and training with different input parameters for all different session are given in Table 4.10.

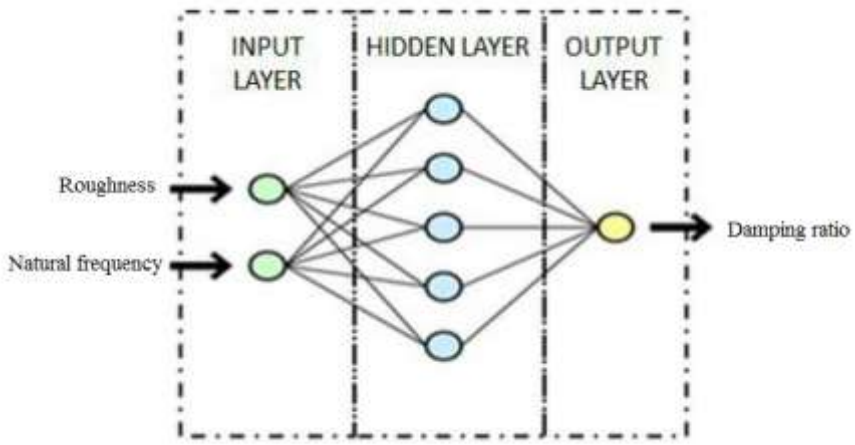

Figure 4.6 Architecture of multilayer neural network system

Table 4.10 Design of neural network and training parameters for all sessions, with two input and one output parameter

Session	# of neurons in input layer	# of neurons in hidden layer	# of neurons in output layer	Learning rate	Momentum coefficient	# of example set used in Training	# of epoch	Root mean Square Error (RMSE)
1	2	20	1	.5	0.006	32	50000	0.006567
2	2	19	1	.6	0.005	32	50000	0.00817
3	2	18	1	.5	0.005	32	50000	0.006785
4	2	16	1	.4	0 .005	32	50000	0.008559
5	2	18	1	.4	0.007	32	50000	0.01053
6	2	19	1	.6	0.006	32	50000	0.0110

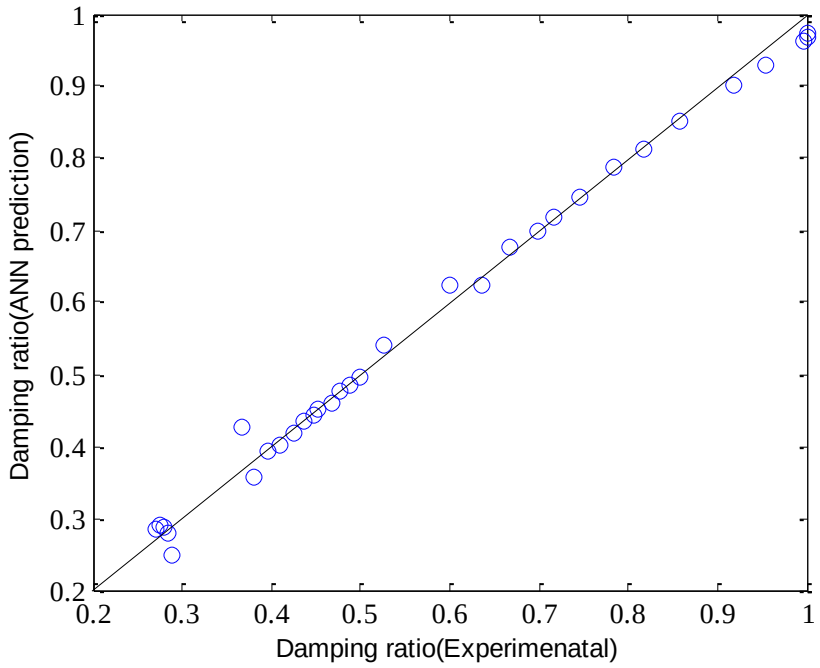

Figure 4.7 Validation curve for experimental and artificial neural network values

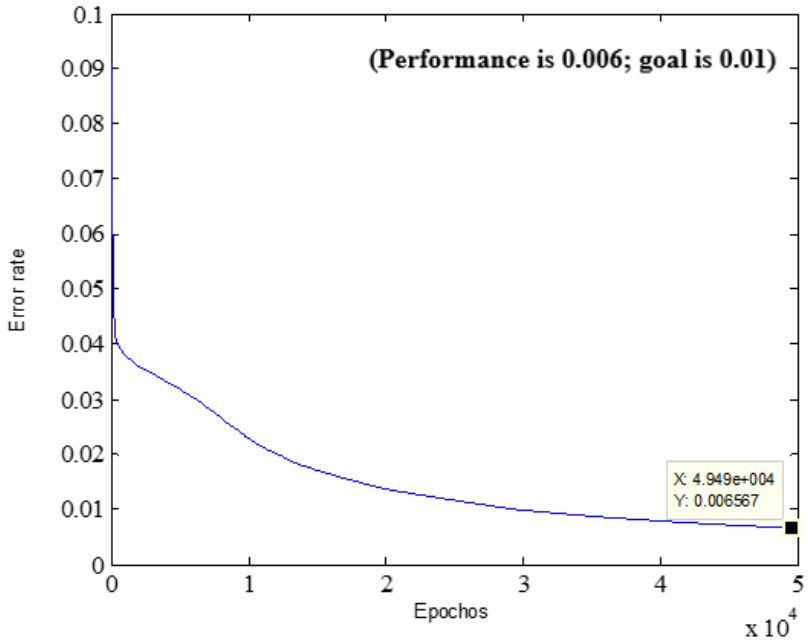

Figure 4.8 Error convergence curve with number of iteration.

Figure 4.7 depicts the validation curve of the experimental and prediction data, which are very much aligned with the ideal prediction curve. Error of the system converging rapidly from 10000 epochs and decreasing to the level of 0.006567 at 50000 iteration. After getting less amount of root mean square error the adjusted weight are ready for predicting new input value of natural frequency and roughness to get new damping ratio value. Finally calculating the error between predicted value and target it was found that the error is 5% which is quite acceptable for the model. Figure 4.9, shown below represents of convergence of error rate with respect to adjustment of synaptic weights. Lastly adjusted weight from Table 4.11 and 4.12 are used for testing further data to predict the damping ratio, which is quite acceptable to adopt the model.

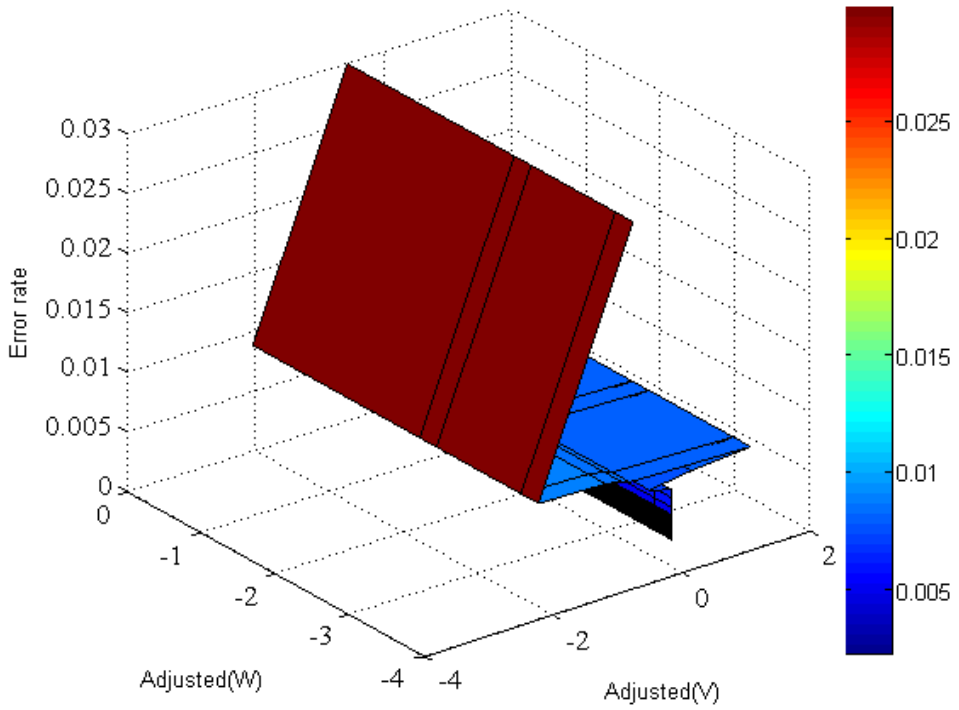

Figure 4.9 Simulation of error rate with respect to adjustment of synaptic weights.

4.4 Summary

From this chapter we conclude that, it is possible to predict damping in layered bolted joint beam structure from many control variables like roughness, torque etc.. From experimental observation an optimum outcome between responses and input parameters are formulate through Taguchi analysis. Then to predict new set of responses and control variable artificial neural network is used. Finally predicated value and experimental values are validated through finding the error, which is acceptably very much low.

Table 4.11 Adjusted hidden weight (*V*)

3.6585	-6.3358
9.1930	-7.3326
5.7880	-8.4852
-3.6245	0.9276
18.4576	-16.8265
3.1344	-1.6168
3.2655	-5.9366
1.1016	-3.8246
1.4712	-4.1761
2.0034	-4.6253
2.5723	-5.1752
3.7203	-6.3770
1.0261	-3.7200
2.4857	-0.9121
1.8373	-4.5307
-1.4040	-1.3734
3.4427	-6.1231
5.3445	-8.0211
3.0924	-5.7733
1.7225	-4.4186

Table 4.12 Adjusted hidden weight(*W*)

-14.0032
6.1547
-14.7455
-11.3392
7.1128
3.5983
-13.6477
-12.9952
-12.9465
-11.6930
-11.7658
-13.6140
-12.3222
3.4570
-13.0264
-12.1913
-13.9520
-14.4339
-13.7429
-12.9830

Chapter-5

Damping analysis of beam with constrained viscoelastic layer

DAMPING ANALYSIS OF BEAM WITH CONSTRAINED VISCOELASTIC LAYER

5.1 Formulation of the problem

There are certain assumption based on which finite element analysis is carried out, and they are given below

(1) The transverse displacement is the equal for all the layers.

(2) Factors like rotary inertia and shear deformation in the constraining layers are insignificant.

(3) Simple theories of elasticity are used.

(4) Slip is absent in between the layers and there is perfect continuity at the interface.

(5) Young's modulus of elasticity of the viscoelastic medium core is negligible as compared to the elastic material.

5.2 Element matrices

The schematic diagram of constrained viscoelastic sandwich structure is shown in Figure 5.1, and the elemental model represent here consist of two nodes with four degree of freedom, which is shown in Figure 5.3.

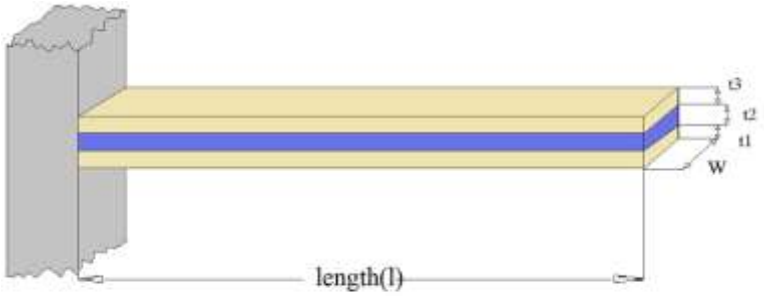

Figure 5.1 Constrained viscoelastic sandwich structure.

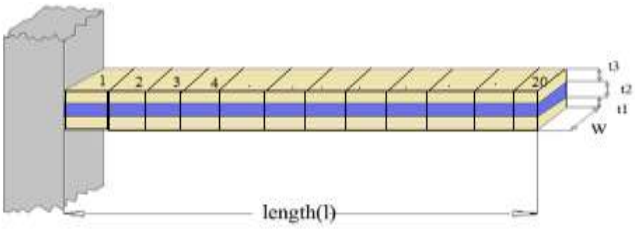

Figure 5.2 Discretization of sandwich structure

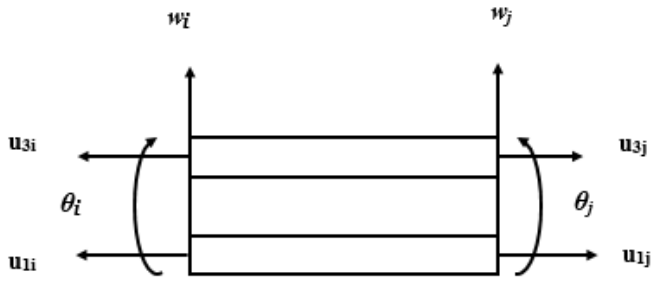

Figure 5.3 Sandwich Beam Element

The nodal displacements are represented as

$$\{\Delta^e\} = \{u_{1i}\ \ u_{3i}\ \ w_i\ \ \Phi_i\ \ u_{1j}\ \ u_{3j}\ \ w_j\ \ \Phi_j\}' \tag{5.1}$$

where *i* and *j* are represents the elemental node numbers. The axial displacement of the constraining layer, the transverse displacement and the rotational angle, can be indicated in terms of nodal displacements and finite element shape functions.

$$u_1 = [N_1]\{\Delta^e\},\ u_3 = [N_3]\{\Delta^e\},\ w = [N_w]\{\Delta^e\},\quad \Phi = [N_w]'\{\Delta^e\} \tag{5.2}$$

where the prime denotes differentiation with respect to axial coordinate *x* and the shape functions are given by

$$[N_1] = [1-\xi\ \ 0\ \ 0\ \ 0\ \ \xi\ \ 0\ \ 0\ \ 0]$$

$$[N_3] = [0\ \ 1-\xi\ \ 0\ \ 0\ \ 0\ \ \xi\ \ 0\ \ 0]$$

and $$[N_w] = [0\ \ 0\ \ (1-3\xi^2+2\xi^3)\ \ (\xi-2\xi^2+\xi^3)L_e\ \ 0\ \ 0\ \ 3\xi^2-2\xi^3\ \ (-\xi^2+\xi^3)L_e] \tag{5.3}$$

where, $\xi = x / L_e$ and L_e is the effective length of the element.

5.2.1 Element stiffness matrices

Potential energy of the element ($U^{(e)}$) is equal to the summation of the potential energy of the constraining layers and viscoelastic layer.

$$U^{(e)} = U_k^{(e)} + U_2^{(e)} \tag{5.4}$$

i. The potential energy of the constraining layers along the axial direction and bending is given as

$$U_k^{(e)} = \sum_{k=1,3}\left[\frac{1}{2}\int_0^{L_e} E_k\, I_k \left(\frac{\partial^2 w}{\partial x^2}\right)^2 dx + \frac{1}{2}\int_0^{L_e} E_k\, A_k \left(\frac{\partial u_k}{\partial x}\right)^2 dx\right] \tag{5.5}$$

Where E_k, A_k and I_k are the modulus of elasticity, cross-sectional area and area rotetional inertia respectively. The symbolizations 1 and 3 represent the lower and upper constraining layer, respectively.

By substituting Eq. (5.2) in to Eq. (5.5), the potential energy of the constraining layers element can be given as

$$U_k^{(e)} = \sum_{k=1,3}\frac{1}{2}\left\{\Delta^{(e)}\right\}\left(\left[K_{ku}^{(e)}\right] + \left[K_{kw}^{(e)}\right]\right)\left\{\Delta^{(e)}\right\} \tag{5.6}$$

where,

$$\left.\begin{aligned}\left[K_{ku}^{(e)}\right] &= \sum_{k=1,3} E_k\, A_k \int_0^{L_e} \left[N_k\right]'^T \left[N_k\right] dx \\ \left[K_{kw}^{(e)}\right] &= \sum_{k=1,3} E_k\, I_k \int_0^{L_e} \left[N_w\right]''^T \left[N_w\right]'' dx\end{aligned}\right\} \tag{5.7}$$

ii. The potential energy store by viscoelastic layer due to shear deformation is written as

$$U_2^{(e)} = \frac{1}{2}\int_0^{L_e} G_2 A_2 \gamma^2 \, dx \tag{5.8}$$

where, A_2 is the area of cross-section and G_2 is known as the complex shear modulus of the viscoelastic layer. The complex modulus of the viscoelastic layer can be stated as $G_2 = G' + G''i$, where G' *is* the shear storage modulus and G'' is known as the loss modulus factor. Core loss factor η is define as the ratio of G''*and* G'*. So* G_2 can be written as $G_2 = G'(1 + \eta\,\mathrm{i})$.

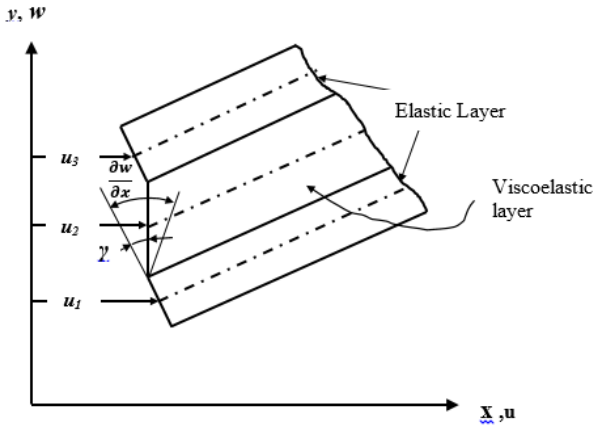

Figure 5.4 Kinematic relations of deflected structure

Referring to Figure (5.4), from the kinematic relationships between the constraining layers, the axial elongation u_2 and shear displacement γ of the viscoelastic layer are given below:

$$u_2 = \frac{u_1 + u_3}{2} + \frac{(t_3 - t_1)}{4}\frac{\partial w}{\partial x} \tag{5.9}$$

$$\gamma = \frac{u_3 - u_1}{t_2} + \frac{(t_1 + 2t_2 + t_3)}{2t_2}\frac{\partial w}{\partial x} \tag{5.10}$$

Substituting Eq. (5.2) in to Equation. (5.9) and (5.10) u_2 and γ can be stated in terms of nodal displacements and shape functions of the elemental body:

$$u_2 = [N_2]\{\Delta^{(e)}\} \tag{5.11}$$

$$\gamma = [N_\gamma] \quad \{\Delta^{(e)}\} \tag{5.12}$$

where,

$$[N_2] = \frac{1}{2}\left([N_1]+[N_3]\right)\frac{(t_3 - t_1)}{4}[N_w]' \tag{5.13}$$

$$[N_\gamma] = \frac{\left([N_3]-[N_1]\right)}{t_2} + \frac{(t_1 + 2t_2 + t_3)}{2t_2}[N_w]' \tag{5.14}$$

Substituting Eq. (5.14) in to Eq. (5.8), the potential energy of the viscoelastic layer is given by

$$U_2^{(e)} = \frac{1}{2}\{\Delta^{(e)}\}^T \left([K_\gamma^{(e)}]\right)\{\Delta^{(e)}\} \tag{5.15}$$

where,

$$[K_\gamma^{(e)}] = G_2 A_2 \int_0^{L_e} [N_\gamma]^T [N_\gamma]\, dx \tag{5.16}$$

From Eq. (5.4) elemental potential energy

$$U^{(e)} = \sum_{k=1,3}\frac{1}{2}\{\Delta^{(e)}\}^T \left([K_{ku}^{(e)}]+[K_{kw}^{(e)}]\right)\{\Delta^{(e)}\} + \frac{1}{2}\{\Delta^{(e)}\}^T \left([K_{2\gamma}^{(e)}]\right)\{\Delta^{(e)}\}$$
$$= \frac{1}{2}\{\Delta^{(e)}\}^T \left([K^{(e)}]\right)\{\Delta^{(e)}\} \tag{5.17}$$

where, the stiffness matrix of the element is,

$$[K^{(e)}] = \sum_{k=1,3}\left([K_{ku}^{(e)}]+[K_{kw}^{(e)}]\right)+[K_{2\gamma}^{(e)}] \tag{5.18}$$

5.2.2 Element mass matrix

Elemental kinetic energy ($T^{(e)}$) is equal to the addition of the kinetic energy of the viscoelastic layer and constraining layers.

$$T^{(e)} = T_k^{(e)} + T_2^{(e)} \tag{5.19}$$

(i) The kinetic energy of the constraining layers is described as

$$T_k^{(e)} = \sum_{k=1,3} \frac{1}{2} \int_0^{L_e} \rho_k A_k \left(\frac{dw}{dx} \right)^2 dx + \frac{1}{2} \int_0^{L_e} \rho_k A_k \left(\frac{du_k}{dx} \right)^2 dx \tag{5.20}$$

where ρ_k is the density of the kth elastic constraining layer.

By replacing Eq. (5.2) in to Eq. (5.20), the kinetic energy of the constraining layers element can be stated as

$$T_k^{(e)} = \sum_{k=1,3} \frac{1}{2} \left\{ \dot{\Delta}^{(e)} \right\}^T \left(\left[M_{ku}^{(e)} \right] + \left[M_{kw}^{(e)} \right] \right) \left\{ \dot{\Delta}^{(e)} \right\} \tag{5.21}$$

where,

$$\left.\begin{aligned} \left[M_{ku}^{(e)} \right] &= \sum_{k=1,3} \rho_k A_k \int_0^{L_e} [N_k]^T [N_k] dx \\ \left[M_{kw}^{(e)} \right] &= \sum_{k=1,3} \rho_k A_k \int_0^{L_e} [N_w]^T [N_w] dx \end{aligned}\right\} \tag{5.22}$$

and, the dot symbolizes differentiation with respect to time t in equation 5.21.

(ii) The kinetic energy of viscoelastic layer is written as

$$T_2^{(e)} = \frac{1}{2} \int_0^{L_e} \rho_2 A_2 \left\{ \left(\frac{dw}{dt} \right)^2 + \left(\frac{du_2}{dt} \right)^2 \right\} dx \tag{5.23}$$

Substituting Eq. (5.2) and Eq. (5.11) in to Eq. (5.23), the K.E of viscoelastic layer is specified by

$$T_2^{(e)} = \frac{1}{2}\left\{\dot{\Delta}^{(e)}\right\}\left[M_2^{(e)}\right]\left\{\dot{\Delta}^{(e)}\right\} \tag{5.24}$$

Where,

$$\left[M_2^{(e)}\right] = \rho_2 A_2 \int_0^{L_e}\left[N_w\right]^T\left[N_w\right]dx + \rho_2 A_2 \int_0^{L_e}\left[N_2\right]^T\left[N_2\right]dx \tag{5.25}$$

The dot means differentiation with respect to time t.

From Eq.5.19, $T^{(e)} = \sum_{k=1,3}\frac{1}{2}\left\{\dot{\Delta}^{(e)}\right\}^T\left(\left[M_{ku}^{(e)}\right] + \left[M_{kw}^{(e)}\right]\right)\left\{\dot{\Delta}^{(e)}\right\} + \frac{1}{2}\left\{\dot{\Delta}^{(e)}\right\}^T\left[M_2^{(e)}\right]\left\{\dot{\Delta}^{(e)}\right\}$

$$T^{(e)} = \frac{1}{2}\left\{\dot{\Delta}^{(e)}\right\}^T\left[M^{(e)}\right]\left\{\dot{\Delta}^{(e)}\right\} \tag{5.26}$$

Where, $\left[M^{(e)}\right] = \sum_{k=1,3}\left(\left[M_{ku}^{(e)}\right] + \left[M_{kw}^{(e)}\right]\right) + \left[M_2^{(e)}\right]$ and $\left[M^{(e)}\right]$ is the elemental mass matrix.

5.3 Equation of motion

The equations of motion for a sandwich beam structure with constrained damping layer exposed to an axial periodic load is formulated by using Hamilton's principle.

$$\delta\int_{t1}^{t2}\left(T^{(e)} - U^{(e)}\right)dt = 0 \tag{5.27}$$

Substituting equation (5.17) and (5.26) in to Eq. (5.27) the element equation of motion for the sandwich beam element are obtained as follows:

$$\left[M^{(e)}\right]\left\{\ddot{\Delta}^{(e)}\right\} + \left[K^{(e)}\right]\left\{\Delta^{(e)}\right\} = 0 \tag{5.28}$$

Assembling mass and stiffness matrices of individual element, the equation of motion for the beam structure is written as

$$[M]\{\ddot{\Delta}\}+[K]\{\Delta\} = 0 \tag{5.29}$$

Where, $\{\Delta\}$ is the global displacement matrix.

If $(\omega_m)^2$ are the distinct eigenvalues of $[M]^{-1}[K]$

$$\omega_m^2 = \omega_{m.R}^2 + i\,\omega_{m.I}^2$$

Modal loss factor of mth mode is

$$\eta_m = \frac{\omega_{mI}{}^2}{\omega_{mR}{}^2} \tag{5.30}$$

Twenty elements are chosen for the beam specimen to calculate modal loss factor. The different values of modal loss factor are obtained by taking different values of core loss factor and core thickness parameter, which is shown in Table 5.1.

Table 5.1 Modal loss factor in finite element analysis

SR No.	Core thickness parameter (*A*)	core loss function (*B*)	mode loss factor (η)
1	0.5	0.3	0.0780
2	0.5	0.5	0.1194
3	0.5	0.8	0.1599
4	0.5	1.1	0.1784
5	0.7	0.3	0.0972
6	0.7	0.5	0.1502
7	0.7	0.8	0.2048
8	0.7	1.1	0.2326
9	0.8	0.3	0.1054
10	0.8	0.5	0.1636
11	0.8	0.8	0.2247
12	0.8	1.1	0.2572
13	1.0	0.3	0.1262
14	1.0	0.5	0.1871
15	1.0	0.8	0.2603
16	1.0	1.1	0.3021

5.4 Taguchi analysis in modal loss factor

The main objective of this section is to provide an accurate method for a predictive model for modal loss factor of sandwich beam structure. Modal loss factor and natural frequency are the important factors for determining the damping of constrained layer viscoelastic structure. So higher modal loss factor gives us a sound sandwich structure for damping purpose, hence effecting correlation between the controls factors are optimized through Taguchi principle. After finding of modal loss factor from finite element formulation, for different parametric condition, the observed data are converted into signal-to-noise ratios. Table 5.2 presented below gives the S/N ratio for different modal loss factor. There are different form of S/N ratio depending on its characteristics. The S/N ratio for maximum modal loss factor coming under larger-is–better characteristic can be calculated as shown in equation 5.31.

$$S/N = -10\log(\sum(1/Y^2)/n) \tag{5.31}$$

where, n is the number of observations and Y is the observed data

Table 5.2 Modal loss factor corresponding S/N ratio

Mode loss factor(η)	S/N ratio
0.0780	-22.1581
0.1194	-18.4599
0.1599	-15.9230
0.1784	-14.9721
0.0972	-20.2467
0.1502	-16.4666
0.2048	-13.7734
0.2326	-12.6678
0.1054	-19.5432
0.1636	-15.7243
0.2247	-12.9679
0.2572	-11.7946
0.1262	-17.9788
0.1871	-14.5585
0.2603	-11.6905
0.3021	-10.3970

Table 5.3 Response table for signal to noise ratios

Level	Core thickness parameter(A)	core loss factor(B)
1	-17.88	-19.98
2	-15.79	-16.30
3	-15.01	-13.59
4	-13.66	-12.46
Delta	4.22	7.52
Rank	2	1

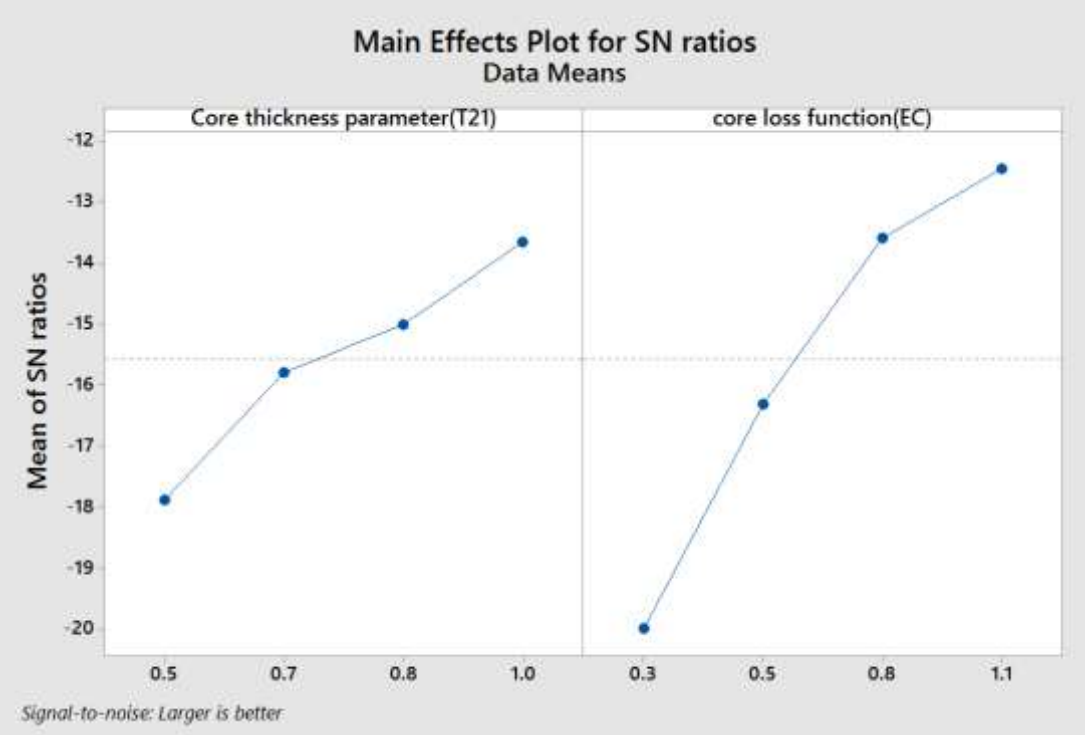

Figure 5.5 Effects of control parameters on Modal loss factors

The S/N ratio response table is given in Table 5.3, from which it can be decided that among all the parameter core loss function is more significant factor followed by core thick ness parameter. It is also concluded from Figure 5.5, that core thickness factor of 1 unit and core loss factor of 1.1 unit gives the maximum condition of modal loss factor

Table 5.4 Analysis of variance (ANOVA) for damping test result

Source	Degree of freedom	Sum of squares	Mean square	F-Value	P-value
Core thickness parameter	3	0.015033	0.005011	25.16	0.00
Core loss factor	3	0.046809	0.015603	78.35	0.00
Error	9	0.001792	0.000199		
Total	15	0.063634			

Different factor affects the modal loss factor into different degree. A better feeling for relative effects of different factors is obtained by decomposition of the variance, which is commonly known as analysis of variance (ANOVA). Table5.4 shows the anova table for modal loss factor response .The important information obtained here is the percentage influence of all factors over responses. Percentage influence(P) value less than 0.0500 indicate the model terms are significant.

In this case core thickness parameter and core loss factor are both significant model terms. But core loss factor is more significant because of its higher variance ratio. So it shows core loss factor has more contribution to modal loss factor.

5.5 Formulation of factors for maximum Modal loss factor

A regression model is proposed in the present work to develop the relationship between the input parameters such as core thickness parameter and core loss factor with the output characteristics such as damping ratio and natural frequency. This model is developed by using popular statistical software SYSTST13. The mathematical formulation to make a correlation among parameters in different order are given below.

1^{st} order $\quad P_f = K_0 + K_1 A + K_2 B$ (5.32)

$$\underline{2^{nd}\ \text{order}}\ P_f = K_0 + K_1A + K_2B + K_3A^2 + K_4B^2 \quad (5.33)$$

where, P_f represents performance of the system

K_i (0, 1, 2, 3 and 4) are model constant

A is core thickness parameter

B core loss factor

$\underline{1^{st}\ \text{order}}$ Modal loss factor (η) = -0.068+0.170A-0.175B (R-sq. 99.4%) (5.34)

$\underline{2^{nd}\ \text{order}}$ Modal loss factor (η) =-0.155+0.246A+0.388B

-0.$051A^2$-0.$151B^2$ (R-sq. 99.7%) (5.35)

The correctness of the correlation is also confirmed as high coefficient of determination (R-sq.) is obtained from equation 5.34 and 5.35 is 99.4% and 99.7%respectively. Therefore the model is quite appropriate to used for the additional predictive purpose.

5.6 Analysis and prediction of modal loss factor using Artificial Neural Network system:

After formulation of modal loss factor of constrained viscoelastic layer in finite element analysis, the result is analysed through an artificial neural network system. Here network consist of three layers.

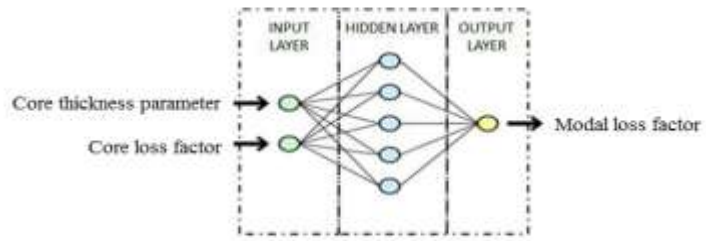

Figure 5.6 The structure of multilayer neural network system

Architecture of multilayer neural network system provided to the input layer as core thickness parameter and core loss factor, some number of neurons is given to hidden layer and modal loss factor as the output layer, which is shown in figure 5.6.

Table 5.5 Design of neural network and training parameters for all sessions, with two input and one output parameter.

Session	# of neurons in input layer	# of neurons in hidden layer	# of neurons in output layer	Learning rate	Momentum coefficient	# of example set used in training	# of epochs	Root mean square error (RMSE)
1	2	12	1	.5	.4	15	50000	0.00536
2	2	12	1	.5	.6	15	50000	0.0062
3	2	8	1	.5	.4	15	50000	0.0062
4	2	8	1	.5	.6	15	50000	0.0063
5	2	16	1	.6	.8	15	50000	0.0077
6	2	12	1	.4	.5	15	50000	0.0058

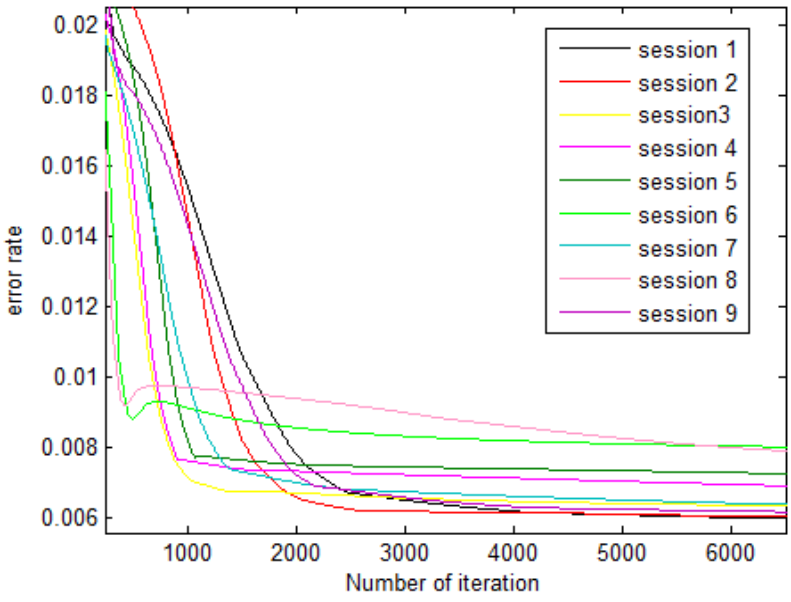

Figure 5.7 Convergence of error in different session

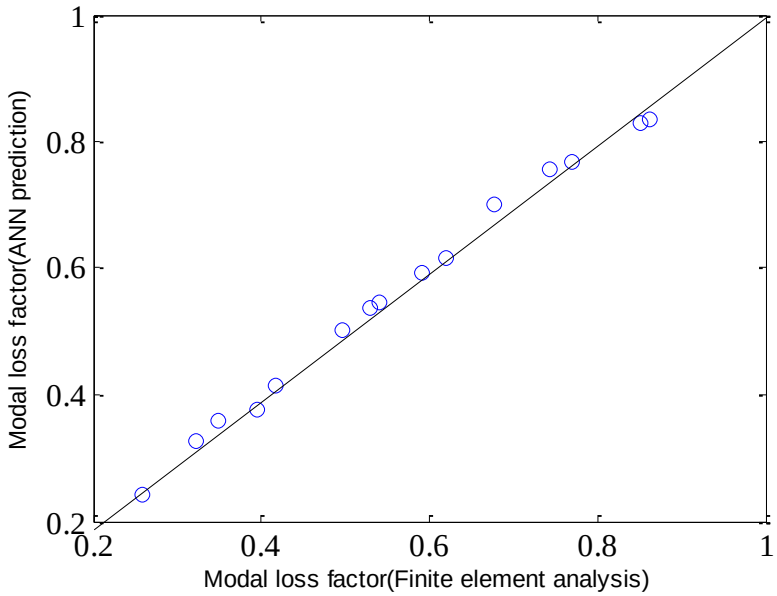

Figure 5.8 validation curve for modal loss factor in between fem analysis and neural network system.

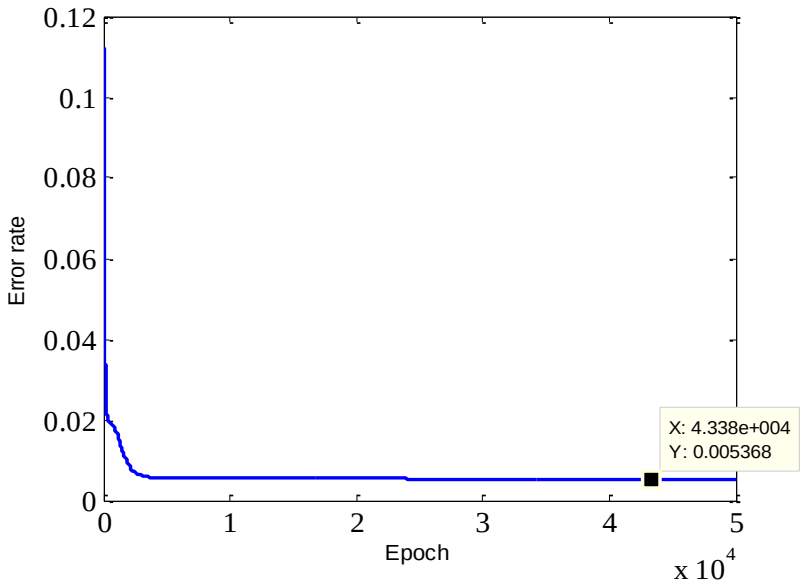

Figure 5.9 Best convergence curve of root mean square error rate with respect to a number of iteration.

After training the whole data base, the system validates the data of modal loss factor with the predicted value of neural network system. Figure 5.9 depict that most of the predicted values are very much nearer to the finite element values. After getting less amount of root mean square error, the adjusted weight from Table 5.10 and 5.11 are ready for predicting new input value of core thickness parameter and core loss factor to get new modal loss factor value. Finally calculating the error between predicted value and the target it is found that the error is 6% which is quite acceptable for the model.

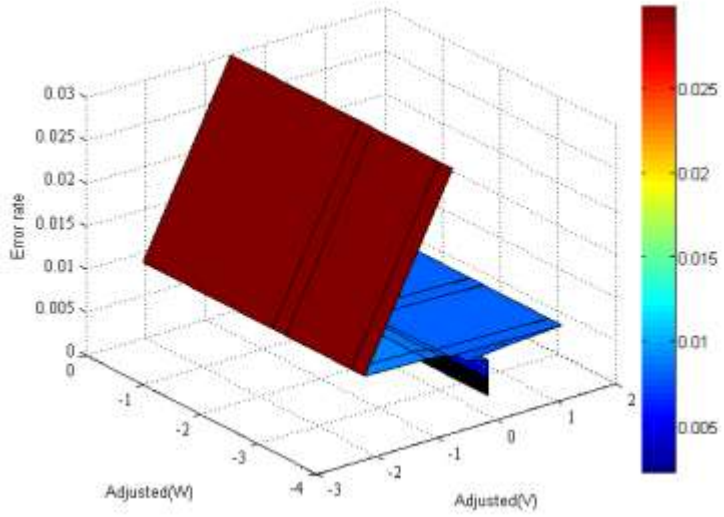

Figure 5.10 Simulation of error rate with respect to adjustment of synaptic weights.

5.7 Summary

From this chapter we conclude that parameters like core thickness factor and core loss factor both play an important role for enhancing the damping in constrained layer. But from the above two parameters core loss factor is more significant because of its higher variance ratio. So it shows that core loss factor has more contribution to modal loss factor than core thickness. To find the optimum modal loss factor a formulation also generated among core thickness parameter and core loss factor in this chapter where as in the previous chapter formulation is created among roughness and torque to find optimum natural frequency and damping ratio in the bolted layered structure.

Table 5.6 Adjusted hidden weight (*V*)

0.43443	0.15480
-0.32041	1.05061
-0.24815	-0.40052
-1.11600	0.62617
0.50238	0.07389
-3.48533	3.08716
0.90315	-0.39990
2.23070	-3.18351
-0.99483	0.48669
-0.58197	-0.00556
1.84787	-2.79478
0.43557	0.15573

Table 5.7 Adjusted hidden weight (*W*)

3.38929
2.95994
-2.70831
-3.92856
3.40927
-4.36524
3.58155
-4.37318
-3.04154
-1.59926
-4.30224
3.64570

Chapter-6

Conclusion and future scope

6

6.1 Conclusions

The main objective of the present work is to estimate the damping capacity of layered beam structure. The damping of jointed layer cantilever beam structure has been studied experimentally taking free vibration condition with different surface roughness in the interface layer of the structure and bolt tightening torque. Based upon the experimental results, Taguchi principle and artificial neural network method have been applied to develop models to predict damping in bolted layered beam structures. The damping capacity in terms of modal loss factor has been studied for sandwich beams with constrained viscoelastic layer. The effect of core loss factor and core thickness on modal loss factor of the sandwich beam has been studied using the finite element based model. Predictive models for damping in sandwich beams have been developed applying Taguchi principle and artificial neural network method. Lastly from the above analysis we conclude that:

- In case of layered beams with bolted joints, the damping capacity increases with increase in surface roughness and higher values of tightening torque of bolts.
- For a sandwich beam with the viscoelastic core the modal loss factor improves with an increase in core loss factor and core thickness.
- Taguchi principle and the artificial neural network can be effectively used to predict accurately damping in bolted layered beams as well as in beams with constrained viscoelastic layer.
- Roughness and torque are both significant model terms in case of bolted layered beams. But roughness is more significant because of its higher variance ratio. So it shows roughness has more contribution to damping ratio.
- Core thickness and core loss factor are both significant model terms in case of beams with constrained damping layer. But core loss factor is more significant because of its higher variance ratio. So it shows that core loss factor has more contribution to modal loss factor than core thickness.

6.2 Scope of future work

The followings aspects can be taken up as extensions of the present work

i) Layered plate with bolted joints and plate with constrained viscoelastic layer.

ii) Finite element modelling of the bolted joint to predict damping.

iii) Nonlinear aspect of the joint may be explored as future work.

References

[1] A. Aherwar, D. Unune, B. Pathri, and J. kishan, "Statistical and Regression Analysis of Vibration of Carbon Steel Cutting Tool for Turning of EN24 Steel Using Design of Experiments," *Int. J. Recent Adv. Mech. Eng.*, vol. 3, no. 3, pp. 137–151, Aug. 2014.

[2] A. Bhimaraddi, "Sandwich beam theory and the analysis of constrained layer damping," *J. Sound Vib.*, vol. 179, no. 4, pp. 591–602, Jan. 1995.

[3] A. Pradhan, "Damping Of Bolted Beams With Unequal Thickness Ratio," M.Tech Research,NIT Rourkela, 2012.

[4] A. S. R. Murty and K. K. Padmanabhan, "Effect of surface topography on damping in machine joints," *Precis. Eng.*, vol. 4, pp. 185–190, Oct. 1982.

[7] B. J. Lazan, "*Damping of Materials and Members in Structural Machanics"*, ed. London: Pergamon Press,1968.

[8] C. D. Johnson and D. A. Kienholz, "Finite Element Prediction of Damping in Structures with Constrained Viscoelastic Layers," *AIAA J.*, vol. 20, pp. 1284–1290, 1982.

[9] C. F. Beards and A. Woowat, "The Control of Frame Vibration by Friction Damping in Joints," *J. Vib. Acoust. Stress Reliab*, vol. 107, pp. 26–32, Jan. 1985.

[10] C. F. Beards, "Damping in structural joints," *Shock Vib. Dig.*, vol. 24, pp. 3–7, 1992.

[11] C. F. Beards, "*Engineering Vibration Analysis with Application to Control Systems"*, ed. Edward Arnold,1995.

[12] C. H. Menq, J. Bielak, and J. H. Griffin, "The influence of micro-slip on vibratory response. Part-I: A new micro slip model," vol.107, pp. 279–293,1996.

[13] C. T. Sun, B. V. Sankar, and V. S. Rao, "Damping and vibration control of unidirectional composite laminates using add-on viscoelastic materials," *J. Sound Vib.*, vol. 139, pp. 277–290, 1990.

[14] C. W. Bert, "Material damping: An introductory review of mathematic measures and experimental technique," *J. Sound Vib.*, vol. 29, no. 2, pp. 129–153, 1973.]

[15] C. H. Menq and J. H. Griffin, "A Comparison of Transient and Steady State Finite Element Analyses of the Forced Response of a Frictionally Damped

Beam," *J. Vib. Acoust. Stress Reliab. Des.*, vol. 107, no. 1, pp. 19–25, Jan. 1985.

[16] "Damping." [Online]. Available: http://www.mfg.mtu.edu/cyberman/machtool/machtool/vibration/damping.html.[Accessed: 16-Jun-2016].

[17] D. K. Rao, "Frequency and loss factors of sandwich beams under various boundary conditions," *Arch. J. Mech. Eng. Sci.*, vol. 20, no. 5, pp. 271–282, Oct. 1978.

[18] E. Cigeroglu, "Nonlinear vibration analysis of bladed disks with dry friction dampers," Middle East Technical University, Ankara, 2006.

[19] E. Cigeroglu, W. Lu, and C. H. Menq, "One-dimensional dynamic microslip friction model," *J. Sound Vib.*, vol. 292, no. 3–5, pp. 881–898, May 2006.

[20] E. E. Ungar, "Loss Factors of Viscoelastically Damped Beam Structures," *J. Acoust. Soc. Am.*, vol. 34, no. 8, pp. 1082–1089, Aug. 1962.

[21] E. H. Dowell and H. B. Schwartz, "Forced response of a cantilever beam with a dry friction damper attached, Part II: Experiment," *J. Sound Vib.*, vol. 91, 1983.

[22] H. Menq, "The influence of microslip on vibratory response, Part II: A comparison with experimental results," *J. Sound Vib.*, vol. 107, no. 2, pp. 295–307, 1986.

[23] J. F. Chen, S. K. Lo, and Q. H. Do, "An Approach to the Classification of Cutting Vibration on Machine Tools," *Information*, vol. 7, no. 1, p. 7, Feb. 2016.

[24] J. Awrejcewicz and P. Olejnik, "Occurrence of stick-slip phenomenon," *J. Theor. Appl. Mech.*, vol. 45, no. 1, pp. 33–40, 2007.

[25] J. H. Wang and W. K. Chen, "Investigation of the Vibration of a Blade With Friction Damper by HBM," *J. Eng. Gas Turbines Power*, vol. 115, no. 2, pp. 294–299, Apr. 1993.

[26] J. P. D. Hartog, "LXXIII. Forced vibrations with combined viscous and coulomb damping," *Lond. Edinb. Dublin Philos. Mag. J. Sci.*, vol. 9, no. 59, pp. 801–817, May 1930.

[27] J. Renninger, "Understanding damping techniques for noise and vibration control," *EAR Div. Cabot Corp.*, 2000.

[30] K. H. Ha, “Exact analysis of bending and overall buckling of sandwich beam systems,” *Comput. Struct.*, vol. 45, pp. 31–40, Sep. 1992.

[31] K. Y. Sanliturk, D. J. Ewins, R. Elliott, and J. S. Green, “Friction Damper Optimization: Simulation of Rainbow Tests,” *J. Eng. Gas Turbines Power*, vol. 123, no. 4, pp. 930–939, Mar. 1999.

[32] L. Gaul and J. Lenz, “Nonlinear dynamics of structures assembled by bolted joints,” *Acta Mech.*, vol. 125, no. 1–4, pp. 169–181, Mar. 1997.

[33] L. Gaul and R. Nitsche, “The Role of Friction in Mechanical Joints,” *Appl. Mech. Rev.*, vol. 54, pp. 93, 2001.

[34] L. Goodman, “Analysis of slip damping with reference to turbine-blade vibration,” *ASME J. Appl. Mech.*, vol. 23, pp. 421–429,1965.

[35] L.Gaul and R. Nitsche, “Friction control for vibration suppression,” *Mech. Syst. Signal Process.*, vol. 14, no. 2, pp. 139–150, Mar. 2000.

[36] M. Avcar and K. Saplioglu, “An Artificial Neural Network Application for Estimation of Natural Frequencies of Beams,” *Int. J. Adv. Comput. Sci. Appl.*, vol. 6, no. 6, 2015.

[37] M. Groper, “Microslip and macroslip in bolted joints,” *Exp. Mech.*, vol. 25, no. 2, pp. 171–174, Jun. 1985.

[38] M. Masuko, Y. Ito, and K. Yoshida, “Theoretical Analysis for a Damping Ratio of a Jointed Cantibeam,” *Bull. JSME*, vol. 16, no. 99, pp. 1421–1432, Sep. 1973.

[39] N. T. Asnani and B. C. Nakra, “Vibration analysis of sandwich beams with viscoelastic core,” *Jr Aeronaut. Soc. India*, vol. 24, no. 1972, pp. 288–294.

[41] P. P. Hujare and A. D. Sahasrabudhe, “Effect of Thickness of Damping Material on Vibration Control of Structural Vibration in Constrained Layer Damping Treatment,” in *Applied Mechanics and Materials*, vol. 592, pp. 2031–2035,2014.

[42] R. A. Ditaranto, “Theory of Vibratory Bending for Elastic and Viscoelastic Layered Finite-Length Beams,” *J. Appl. Mech.*, vol. 32, pp. 881, 1965.

[43] R. A. Ibrahim, “Friction-Induced Vibration, Chatter, Squeal, and Chaos, Part II: Dynamics and Modeling,” *Appl. Mech.*, vol. 47, pp. 227, 1994.

[44] R. Ying, “The analysis and identification of friction joint parameters in the dynamic response of structures,” Imperial College, University of London, UK.

[45] R. Yuan, Q. Zhou, Q. Zhang, and Y. Xie, "Fractal Theory and Contact Dynamics Modeling Vibration Characteristics of Damping Blade," *Adv. Math. Phys.*, pp. e549430, Apr. 2014.

[46] R. Zhou and M. Crocker, "Effects of Thickness on Damping in Foam-filled Honeycomb-core Sandwich Beams."[Online]. Available:http://sem-proceedings.com/25i/sem.org-IMAC-XXV-s41p04-Effects-Thickness-Damping-Foam-filled-Honeycomb-core-Sandwich-Beams.pdf. [Accessed: 07-Aug-2015].

[47] S. Chen and A. Sinha, "Probabilistic Method to Compute the Optimal Slip Load for a Mistuned Bladed Disk Assembly With Friction Dampers," *J. Vib. Acoust.*, vol. 112, no. 2, pp. 214–221, Apr. 1990.

[48] S. Rajasekaran and G. A. V. Pai, Neural Networks, Fuzzy Logic and Genetic Algorithm: Synthesis and Applications. PHI Learning Pvt. Ltd., 2003.

[49] S. S. Abuthakeer, P. V. Mohanram, and G. M. Kumar, "Prediction and Control of Cutting Tool Vibration in Cnc Lathe with Anova and Ann," *Int. J. Lean Think.*, vol. 2, no. 1, pp. 1–23, Jun. 2011.

[50] S. W. Hansen and R. D. Spies, "Structural damping in laminated beams due to interfacial slip," *J. Sound Vib.*, vol. 204, no. 2, pp. 183–202, Jul. 1997.

[51] U. N. L. Gaul, "Nonlinear Vibration Damping of Structures with Bolted Joints," 1994.

[52] U. Olofsson and L. Hagman, "A model for micro-slip between flat surfaces based on deformation of ellipsoidal elastic bodies," *Tribol. Int.*, vol.30, pp. 599–603,1997.

[53] W. de S. Clarence, *Vibration Damping, Control, and Design*, ed. Boca Raton: CRC Press, Taylor and Francis Group LLC, 2004.

[54] W. de S. Clarence, *Vibration: Fundamentals and Practice*, Boca Raton: CRC Press LLC, 2000.

[55] W. Lu, "Modeling of microslip friction and design of frictionally constrained turbine blade systems, PhD Thesis," The Ohio State University, 2001.

[56] W. Sextro, *Dynamical Contact Problems with Friction*. Berlin, Heidelberg: Springer Berlin Heidelberg, 2007.

[57] W. Thomson, *Theory of Vibration with Applications*. CRC Press, 1996.